

# NEWSLETTER

ADVANCING TO NEW HORIZONS

JAN - MAR 2023  
VOLUME 2, ISSUE 1



# NEWSLETTER TEAM

## EDITORS

***Dr. Priyanka Gupta***

Medical Physicist (NM),  
Department of Nuclear Medicine,  
AIIMS, New Delhi

***Dr. Rakhee Vatsa***

Scientific Officer-D,  
Department of Nuclear Medicine,  
ACTREC, TMC, Navi Mumbai

## EDITORIAL TEAM MEMBERS

***Mr. Dinesh Rawat***

Scientific Officer-D,  
Department of Nuclear Medicine,  
ACTREC, TMC, Navi Mumbai

***Mrs. Pooja Dwivedi***

Scientific Officer-D,  
Department of Nuclear Medicine,  
ACTREC, TMC, Navi Mumbai

***Dr. Nivedita Rana***

Nuclear Medicine Physicist,  
Department of Nuclear Medicine,  
PGIMER, Chandigarh

***Ms. Lavanya K***

Medical Physicist (NM),  
Department of Nuclear Medicine,  
AIIMS, Mangalagiri, Andhra Pradesh

***Mr. Naresh Kumar***

PhD Scholar,  
Department Of Nuclear Medicine,  
AIIMS, New Delhi

***Mr. Navneet Kumar***

Technical Assistant,  
Department of Nuclear Medicine,  
AIIMS, Bhubaneswar, Odisha

# LETTER FROM EDITORS

The *Nuclear Medicine Physicists Association of India* (NMPAI) was established in 2007 to promote, protect, and safeguard the interests and future of the Nuclear Medicine Physicists/Technologists fraternity and fulfill its duties towards society. As of now, we have more than 400 members and still growing. NMPAI is managed by a team comprising a president, secretary, treasurer, and six executive committee members, elected by the life members of NMPAI once in two years. Society takes pride in completing fifteen years since inception and seeks to grow leaps and bounds, both academically and socially, in the near future with the continuous efforts of our eminent members/scientists, colleagues, and friends.

As a small step forward in academics, we have started a quarterly newsletter of NMPAI. To date, there has been no official publication of NMPAI. With this quarterly newsletter being the first of its kind, we hope to strengthen our academic association. Research articles, literature reviews, and write-ups related to radiochemistry, instrumentation, radiation safety, imaging, image processing, dosimetry, and software have been the entrees in the newsletter. A dedicated column for advances in nuclear medicine has also been introduced recently.

The *newsletter's first issue* was released last year in 2022, during *Nuclear Medicine Week*, celebrated in India during the *last week of October* (26-31 October). It was a huge success and received appreciation from one and all.

It is truly said that the first step is always the hardest. And in this first step, the entire editorial team worked tirelessly to make it happen. The Executive Committee of NMPAI and the CNMST team also extended their wholehearted support, help, and valuable input to make it a reality. To maintain the continuum, we will come up with quarterly newsletter issues.

Finally, we would like to convey special appreciation and gratitude to all the contributors and readers of the NMPAI newsletter, without whom, it would not have been possible. We encourage and request that you maintain the same enthusiasm for participation and also send us your valuable feedback and ideas for further improvement of your newsletter.

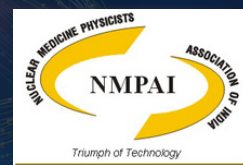


**Dr. Priyanka Gupta**



**Dr. Rakhee Vatsa**

# NUCLEAR MEDICINE PHYSICISTS ASSOCIATION OF INDIA



## EXECUTIVE COMMITTEE

**President:** *Mr. Rajnath K Jaiswar*  
Scientific Officer and RSO  
Department of Nuclear Medicine and PET-CT,  
Bombay Hospital and Medical Research Centre  
Mumbai, India.

**Secretary:** *Mr. Sachin Tayal*  
Scientific Officer-E  
Department of Nuclear Medicine,  
MPMMCC, Varanasi

**Treasurer:** *Mr. Manoj Kumar H Chauhan*  
Scientific Officer-C  
Department of Nuclear Medicine,  
ACTREC, TMC Navi Mumbai

---

## MEMBERS

*Mr Prathamesh Rajai*  
Senior Nuclear Medicine Technologist,  
Institute of Nuclear Medicine,  
University College London Hospital,  
Euston Road, London, UK

*Dr. Priyanka Gupta*  
Medical Physicist (NM),  
Department of Nuclear Medicine,  
AIIMS, New Delhi

*Mrs. Sneha Mithun*  
Scientific Officer-D,  
Department Of Nuclear Medicine,  
Tata Memorial Hospital, Mumbai

*Dr. Rakhee Vatsa*  
Scientific Officer-D,  
Department of Nuclear Medicine,  
ACTREC, TMC, Navi Mumbai

*Dr. Ankit Watts*  
Nuclear Medicine Physicist,  
Department of Nuclear Medicine,  
PGIMER, Chandigarh

*Mr Sukhvinder Singh*  
Scientific Officer-C,  
Department of Nuclear Medicine,  
HBCHRC, Mullanpur, Punjab

# COUNCIL OF NUCLEAR MEDICINE SCIENCE AND TECHNOLOGY



## GOVERNING COUNCIL

**Chairman :** *Dr. Subash Chand Kheruka*  
Consultant, Medical Physics (NM)  
Department of Radiology & Nuclear Medicine  
Sultan Qaboos comprehensive for Cancer  
care and research center,  
Muscat, Oman.

**Vice Chairman :** *Mr. Surya Mishra*  
RSO & Scientific Officer  
School of Life Sciences  
Jawaharlal Nehru University, New Delhi

**Registrar :** *Mrs. Sneha Mithun*  
Scientific Officer-D  
Department of Nuclear Medicine,  
Tata Memorial Hospital, Mumbai

**Secretary :** *Dr. Amit Nautiyal*  
Clinical Scientist (Nuclear Medicine Physics)  
Department of Medical Physics, Minerva House  
University Hospital Southampton

**Treasurer :** *Mr. Anindya Roy*  
Senior Nuclear Medicine Physicist cum RSO  
North city hospital and diagnostics, Kolkata

- Members :**
- 1.** *Dr. Shivanand Bhushan*  
Associate Professor  
Department of Nuclear Medicine  
MCHP, MAHE, Manipal
  - 2.** *Dr. Sarika Sharma*  
Nuclear Medicine Physicist  
Department of Nuclear Medicine,  
PGIMER, Chandigarh
  - 3.** *Dr. Anil K. Pandey*  
Additional Professor  
Department of Nuclear Medicine  
AIIMS, New Delhi

**Ex officio Member :** *Mr. Rajnath Jaiswar* (President NMPAI)

## EDUCATIONAL COMMITTEE

**Chairman :** *Dr. Ashish Kumar Jha*  
Scientific Officer-E  
Department of Nuclear Medicine,  
Tata Memorial Hospital  
Mumbai, India.

**Vice Chairman :** *Dr. Priyanka Gupta*  
Medical Physicist (NM)  
Department of Nuclear Medicine,  
AIIMS, New Delhi

**Secretary :** *Dr. Amit Nautiyal*  
Clinical Scientist (Nuclear Medicine Physics)  
Department of Medical Physics, Minerva House  
University Hospital Southampton

- Members :**
- 1.** Mrs. Sibi Oommen  
Assistant Professor (Sr. Scale),  
Department of Nuclear Medicine,  
Manipal college of Health Professions, Manipal
  - 2.** Dr. Sanjay Bharati  
Associate Professor & Head,  
Department of Nuclear Medicine,  
Manipal college of Health Professions, Manipal
  - 3.** Mr. Dibya Prakash  
Nuclear Medicine Physicist and RSO,  
Founder NM Solutions, Ghaziabad



# NMPAICON - 2023



## 7<sup>th</sup> ANNUAL CONFERENCE OF NUCLEAR MEDICINE PHYSICISTS ASSOCIATION OF INDIA

**"An irresistible rise post pandemic, Commitment to Excellence"**

**(4<sup>th</sup> - 5<sup>th</sup> FEB, 2023)**



**DEPARTMENT OF NUCLEAR MEDICINE & MOLECULAR IMAGING  
MAHAMANA PANDIT MADAN MOHAN MALAVIYA CANCER CENTER (MPMCC),  
VARANASI**

# 4th FEBRUARY (DAY 1)

8:00 ONWARDS: REGISTRATION  
8:30 – 9:30: SESSION – 1

## ADVANCEMENT IN INSTRUMENTATION & RADIATION PHYSICS

CHAIRPERSON: DR. ANIL PANDEY, DR. ISHITA SEN & MS. SHYAMALA BEMBEY

| TIME SLOT   | NAME OF SPEAKER     | TOPIC   |
|-------------|---------------------|---|
| 08:30-08:45 | MR. DINESH KUMAR    | PLANNING OF NUCLEAR MEDICINE DEPARTMENT                       |
| 08:45-09:00 | DR. AJAY CHITKARA   | RADIATION DETECTORS, ADVANCEMENTS AND THEIR APPLICATION IN NM |
| 09:00-09:15 | DR. SUBHASH KHERUKA | QC OF SPECT   |
| 09:15-09:30 | MR. DIBYA PRAKASH   | IMAGE FUSION AND ITS CHALLENGES                               |

| TIME SLOT   | EVENT                                   |
|-------------|---|
| 09:50-10:00 | WELCOME ADDRESS (PRESIDENT, NMPAI)      |
| 10:00-10:20 | LAMP LIGHTNING AND PRAYER               |
| 10:20-10:30 | ADDRESS BY THE PATRON, DR V. RANGARAJAN |
| 10:30-10:40 | DIRECTOR'S ADDRESS (CHIEF PATRON)       |
| 10:40-10:50 | CHIEF GUEST- INAUGURAL SPEECH           |
| 10:50-11:00 | ADDRESS BY GUEST OF HONOR               |
| 11:00-11:05 | VOTE OF THANKS (SECRETARY, NMPAI)       |
| 11:05-11:15 | ABSTRACT BOOK & NEWSLETTER              |

11:15 – 11:30 : HIGH TEA

| TIME SLOT   | NAME OF SPEAKER | TOPIC  |
|-------------|-----------------|--|
| 11:30-11:45 | DR. M R PILLAI  | AN OVERVIEW OF PROJECT PLANNING OF A MEDICAL CYCLOTRON |
| 11:45-12:00 |                 | AERB AWARENESS PROGRAM                                 |

12:00 – 13:00: ORATION ERNEST LAWRENCE

CHAIRPERSON: MR. RAJNATH JAISWAR, MR. SACHIN TAYAL

13:00 – 14:00: LUNCH

14:00 – 15:00: SESSION – 2

## CYCLOTRON BASED PRODUCTION OF NOVEL RADIONUCLIDES

CHAIRPERSON: DR. PANKAJ TANDON & DR. SANJAY GAMBHIR

| TIME SLOT   | NAME OF SPEAKER                       | TOPIC  |
|-------------|---------------------------------------|--|
| 14:00-14:15 | DR. MUKESH PANDEY, MAYO CLINIC        | CYCLOTRON BASED PRODUCTION OF RADIO METALS IN LIQUID TARGETS: BENCH TO BEDSIDE |
| 14:15-14:30 | DR. MANISH DIXIT                      | PRODUCING RADIO METAL IN SOLID TARGET USING 18MEV CYCLOTRON: OUR EXPERTISE     |
| 14:30-15:00 | DR. JEONGHOON PARK KAERI, SOUTH KOREA | ZR89 AND CU64 PRODUCTION WITH RFT-30 CYCLOTRON                                 |

15:00 – 15:45: SESSION-3

## NOVEL DIAGNOSTIC & THERAPEUTIC RADIOPHARMACY

CHAIRPERSON: DR. JAYA SHUKLA, DR. ARCHANA MUKHERJEE & DR. MEERA VENKATESH

| TIME SLOT   | NAME OF SPEAKER       | TOPIC  |
|-------------|-----------------------|--|
| 15:00-15:15 | DR. N RAMAMOORTHY     | RADIOPHARMACEUTICAL FOSTERING AVAILABILITY AND STRATEGIES  |
| 15:15-15:30 | DR. AJISH             | STORY OF PEPTIDE BASED PSMA TARGETING LIGAND   |
| 15:30-15:45 | DR. RAVITEJA NANABALA | F-18 RADIOPHARMACEUTICALS PRODUCTION AND LABELLING STRATEGIES OF SMALL MOLECULES AND BIOMOLECULES: |

15:45 – 16:45: SESSION – 4

## DOSIMETRY

CHAIRPERSON: DR. PRIYANKA GUPTA & DR. ANKUR PRUTHI

| TIME SLOT   | NAME OF SPEAKER     | TOPIC   |
|-------------|---------------------|---|
| 15:45-16:00 | DR. ANKIT WATTS     | PET DOSIMETRY   |
| 16:00-16:15 | MR. NARESH KUMAR    | DOSIMETRY ASPECTS AND DOSE DELIVERY OF 90Y-SIR SPHERES TARE IN HEPATOCELLULAR CARCINOMA |
| 16:15-16:30 | DR. AMIT NAUTIYAL   | DOSIMETRY IN NUCLEAR MEDICINE THERAPY: PRACTICAL CONSIDERATIONS                         |
| 16:30-16:45 | MS. KOMALPREET KAUR | SPECT QUANTIFICATION  |

16:45 – 17:00: EVENING TEA

17:00 – 18:30: ORAL PAPER & E-POSTER PRESENTATIONS

JUDGES: (MR. OMA SHANKAR, MR. NEERAJ SHARMA, DR. PRIYANKA GUPTA)

19:30 ONWARDS DINNER

# 5th FEBRUARY (DAY 2)

08:30-09:30: GBM  
09:30 – 10:15: SESSION – 5

## DIAGNOSTIC & THERAPEUTIC CLINICAL NUCLEAR MEDICINE

CHAIRPERSON: DR. P. K. PRADHAN & DR. VISHU VIJAYANT CHAUHAN

| TIME SLOT   | NAME OF SPEAKER       | TOPIC   |
|-------------|-----------------------|---|
| 09:30-09:45 | DR. SAYAK CHAUDHURY   | PET-CT ACQUISITION- WHAT MAKES A GOOD IMAGE?                        |
| 09:45-10:00 | DR. ARCHANA MUKHERJEE | NUCLEAR IMAGING OF BACTERIAL INFECTION: PAST AND PRESENT SCENARIO"  |
| 10:00-10:15 | DR. PARUL THAKRAL     | SYNTHESIS, BIODISTRIBUTION AND CLINICAL EFFICACY OF GA68 TRIVEHEXIN |

10:15 – 11:15: SESSION – 6

## RADIATION SAFETY & RADIATION BIOLOGY

CHAIRPERSON: DR. SHAMIM AHMED SHAMIM & DR. NANDINI PANDIT

| TIME SLOT   | NAME OF SPEAKER   | TOPIC   |
|-------------|-------------------|---|
| 10:15-10:30 | DR. PANKAJ TANDON | THE POTENTIAL AND HURDLES OF TARGETED ALPHA THERAPY       |
| 10:30-10:45 | DR. SANJAY BHARTI | RECEPTOR BASED TARGETING OF THERAPEUTIC RADIONUCLIDES     |
| 10:45-11:00 | MS. PRIYA SHARMA  | CRITICAL ORGANS AND ORGAN DOSES IN RADIONUCLIDE THERAPIES |
| 11:00-11:15 | MS. AMANDEEP KAUR | ACUTE RADIATION EFFECTS ON MAJOR ORGAN SYSTEM             |

11:15 – 11:30 – HIGH TEA

| TIME SLOT     | NAME OF SPEAKER  | TOPIC                  |
|---------------|------------------|------------------------|
| 11:30 – 11:45 | MR. PRANAV RATNA | "INDUSTRIAL TALK"      |
| 11:45 – 12:00 |                  | AERB AWARENESS PROGRAM |

12:00 – 13:00: ORATION HAL ANGER

CHAIRPERSON: MR. RAJNATH JAISWAR, MR. SACHIN TAYAL

13:00 – 14:00: LUNCH

14:15 – 15:00: SESSION – 7

## MATHEMATICAL MODELING & AI

CHAIRPERSON: DR. VENKATESH RANGARAJAN & MR. RAJNATH JAISWAR

| TIME SLOT   | NAME OF SPEAKER   | TOPIC   |
|-------------|-------------------|---|
| 14:15-14:30 | DR. NIVEDITA RANA | BASICS OF IMAGE PROCESSING IN NM USING PYTHON               |
| 14:30-14:45 | MS. SNEHA MITHUN  | NATURAL LANGUAGE PROCESSING FROM SCRATCH FOR PHYSICIST      |
| 14:45-15:00 | MS. POOJA DWIVEDI | RECENT ADVANCES IN PET RECONSTRUCTION AND APPLICATION OF AI |

15:00 – 16:15: SESSION – 8

## CYCLOTRON PHYSICS & RADIOCHEMISTRY

CHAIRPERSON: DR. PILLAI & DR. PRADIP CHAUDHARI

| TIME SLOT   | NAME OF SPEAKER            | TOPIC  |
|-------------|----------------------------|--|
| 15:00-15:15 | MR. SANDEEP SHARMA         | ION SOURCE   |
| 15:15-15:30 | DR RAJEEV KUMAR            | CYCLOTRON MAINTENANCE  |
| 15:30-15:45 | DR. PARDEEP KUMAR          | F18 RADIOCHEMISTRY-FOCUS ON DEVELOPING RADIOTRACER TARGETING NEURO RECEPTORS |
| 15:45-16:15 | PROF. CLEMENS DECRISTOFORO | GMP  |

16:15-17:15: SESSION -9

## CHALLENGES IN NUCLEAR MEDICINE

CHAIRPERSON: MR. ANINDYA ROY & MR. SAMRENDHU SINHA

| TIME SLOT   | NAME OF SPEAKER   | TOPIC  |
|-------------|-------------------|--|
| 16:15-16:30 | MR SAYAN DAS      | STRUCTURE ELUCIDATION  |
| 16:30-16:45 | MR. VIKRANT KUMAR | CT DOSE ESTIMATION   |
| 16:45-17:00 | MR. NAVNEET KUMAR | COMMISSIONING OF A DIGITAL READY PET-CT AT A TERTIARY CARE HOSPITAL                |
| 17:00-17:15 | MR. NEERAJ SHARMA | CHALLENGES & MANAGEMENT OF RUNNING THE NUCLEAR MEDICINE DEPARTMENT IN REMOTE AREAS |

17:15-17:30: VALEDICTORY FUNCTION

17:30 – 18:00: HIGH TEA

# ERNEST LAWRENCE ORATION



## **Mrs. Bhakti Shetye**

Scientific Officer - G  
Department of Nuclear Medicine,  
TMH, Mumbai

In 1989, a fresh postgraduate student of M.Sc. analytical chemistry, she joined Tata Memorial Hospital (TMH) as a scientific assistant B. She got posted at the TMH gamma camera unit installed at Radiation Medicine Centre (RMC). Her journey in nuclear medicine began on 19th June, 1989. Being from chemistry background, nuclear medicine was a new and exciting field for her. Under the guidance of her RMC's seniors Mr. Ramnathan, Dr. PS Soni, and her colleague Dr. B Malpani, she commenced her journey in nuclear medicine by acquainting new acquisition protocols and processing of the acquired data. During the journey of 33 years in RMC and TMH, she got the opportunity to familiarise and master the modalities that has been used in nuclear medicine. Her diverse experience includes handling of rectilinear scanner, rectilinear photo scanner, whole body scanner, first scintillation gamma camera, SPECT gamma camera, dual head gamma camera, first PET scanner installed in India at RMC, first CT-simulator and SPECT-CT installed at TMH. She has witnessed both old and new era of nuclear medicine imaging technology.

In 1991-92, with the support of Dr. AM Samuel, Head RMC, and as a sponsored candidate from TMH, she achieved her qualification as radiation professional (DMRIT) and radiation safety officer certification from AERB. At RMC her academic interest got nurtured by participating in programmes of DMRIT and DRM by delivering lectures and conducting practicals. She has got working experience of 15 years in an institution that is considered as an alma mater of nuclear medicine in India.

Since the inception of separate nuclear medicine department (2004) at TMH, she has played the versatile role of radiochemist, nuclear medicine technologist, and radiation safety officer. She has been a smooth administrator in one of the busiest and leading department in the country. Being a chemist, her research work mainly involves the development of in-house prepared radiopharmaceuticals. She has been actively involved in departmental labeling and quality control program with radionuclides including  $^{177}\text{Lu}$ ,  $^{68}\text{Ga}$ ,  $^{225}\text{Ac}$ . She has played important role in the clinical trial program conducted at Tata Memorial Hospital.

She is actively involved in academic work at TMH as an administrator, examiner, and lecturer. She is a recognized post graduate teacher of Homi Bhabha National Institute (HBNI), a deemed university. She has tremendous contribution in the academic programs conducted at TMH which includes Post Graduate Diploma in Fusion Imaging Technology (PGDFIT) from 2014-2020 under HBNI and the presently running post graduate course (M.Sc.) in Nuclear Medicine and Molecular Imaging Technology (HBNI). With academic experience of more than 30 years she has imparted knowledge to many generations of students.



# HAL ANGER ORATION



***Dr. Chandrasekhar Bal***

Professor & Head of Department,  
Department of Nuclear Medicine,  
AIIMS, NEW DELHI

Dr. Chandrasekhar Bal pursued his MBBS from Utkal University and graduated in 1984. He is one of the few faculty members who has pursued a dual post-graduation degree in basic science (MD, Biophysics) and Nuclear Medicine (DNB, DRM). He set foot as an Assistant Professor at the Department of Nuclear Medicine, AIIMS, New Delhi, in 1991 and is currently the Professor and Head of the Department.

We all do basic or applied science research to quench our inquisitive minds or help humanity solve a few problems. When applied research changes the management globally, it is laudable. Following this approach, the pioneer research work led by Dr. Bal at AIIMS, New Delhi, in the field of thyroid cancer, leads to a change in the management of patients worldwide. Dr. Bal's research brought the optimal dose of radioiodine  $^{131}\text{I}$  to just 30 mCi for remnant thyroid cancer ablation. This outcome has saved millions of dollars in purchasing radioiodine and saved patients from unnecessary whole-body radioiodine exposure. It has also prevented environmental hazards from excess radioactive iodine going to sewerage. And most importantly, patients can be treated with radioiodine on an outpatient basis, with no hospitalization necessary. This work has also been accepted in the 2015 ATA Guidelines for managing differentiated thyroid carcinoma.

Dr. Bal has established several benchmarks in Oncology in India. He believes in adopting modern treatment methods and has successfully performed various first-time procedures in radionuclide therapies. He is also the pioneer of peptide receptor radionuclide and alpha radionuclide therapy in India. He has been recognized with several awards. A few of the landmark research awards include SNMMI 2022 and 2021 Henry N. Wagner, Jr., MD, Best International Abstract Award; ICPO Maurits W Geerlings Next Generation Award 2022 at 6th Theranostic World Congress; EANM 2019 Springer Prize for Best Paper; Young Scientist Award 2018 of the Japanese Society of Nuclear Medicine; SNMMI 2018 Indo-American Young Investigator Award; SNMMI 2017 Young Professional award; World Theranostics Conference Award 2016 at Melbourne, Australia; AIIMS Excellence Award in Clinical Research in the year 2021, 2020, 2017 and 2015; Prof. RD Lele Oration Award ANMPI 2012; Brig. SK Majumdar Memorial Oration Award 2003. He has more than 500 publications with total citations of 8016.

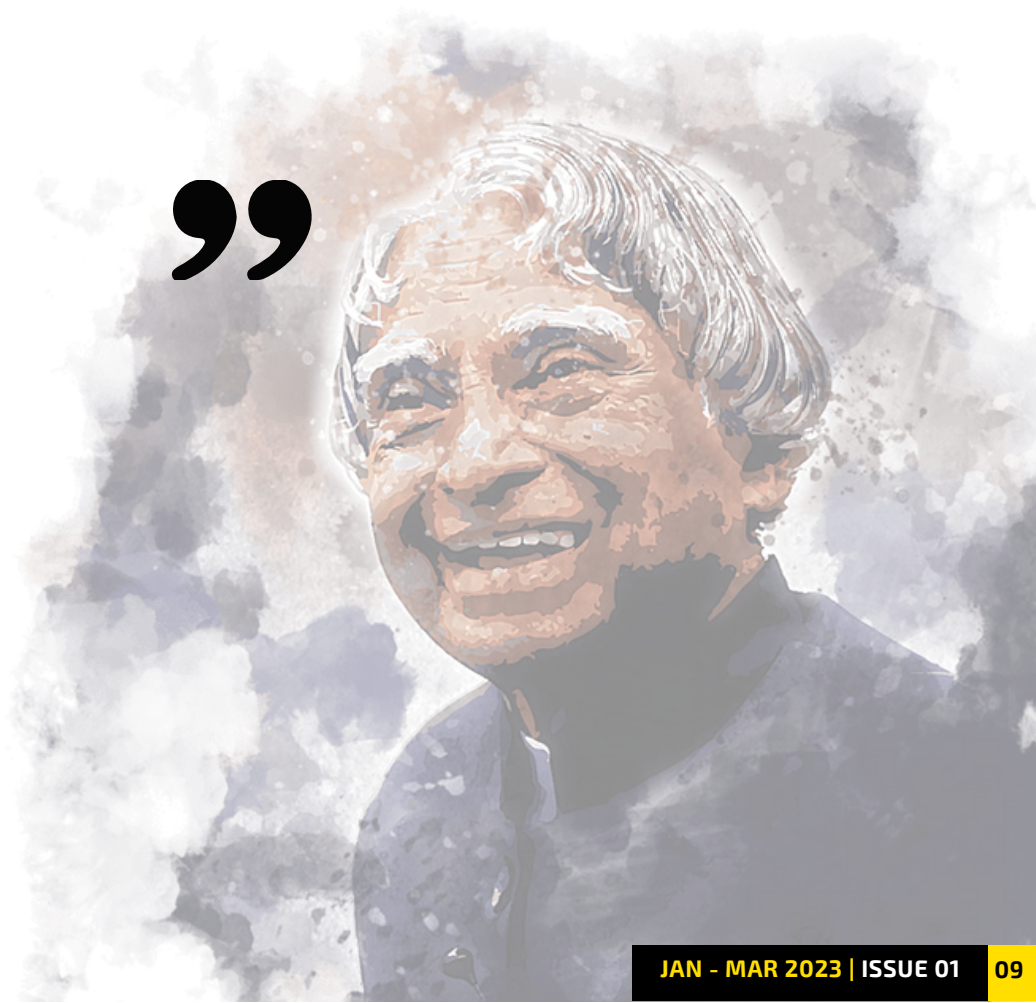
Dr. Bal, not only, has many accolades as a researcher and a clinician, but as a teacher and educator has guided hundreds of students in the DM (Therapeutic Nuclear Medicine), MD and MSc NMT programs at AIIMS, New Delhi. Due to his outstanding contributions to the field, the Indian Nuclear Medicine program has plummeted across many a levels ahead to receive International recognitions.

“

**DREAM IS NOT THAT  
WHICH YOU SEE WHILE  
SLEEPING. IT IS  
SOMETHING THAT DOES  
NOT LET YOU SLEEP.**

**A.P.J. ABDUL KALAM**

”



# NEWSLETTER

## CONTENTS

### 26 Radiation Survey

An Institutional experience of surveying Delay Tank Facility

### 31 Re-188 Radiopharmacy

Reducing elution volume using Silver Ion-exchange resin

### 34 Purification

Cost-effective, single step purification method for radio-labelled small peptides

### 37 Establishing Reference

Reference values for Whole Gut transit scintigraphy using Tc-99m-Sulfur Colloid Liquid Meal

### 46 Crosswords

Brainstorming expected

### 47 Upcoming Events

National Events

### 48 Upcoming Events

International Events

### 11 AUGER ELECTRONS

Opening new realms in Therapy



### 18 SCINTILLATION DETECTORS

Evolution & advancements



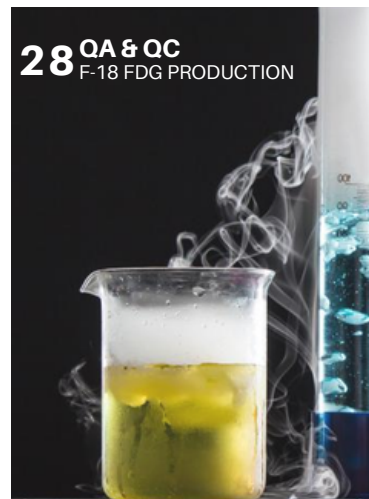
### 43 DIGITAL SPECT-CT

Recent Advances



### 28 QA & QC

F-18 FDG PRODUCTION



### 23 RADIATION PROTECTION

Auxillary Staff Safety

### 14 TOF PET

Principles, History & Advancements



## VOLUME 2 ISSUE 1 JAN-MAR 2023

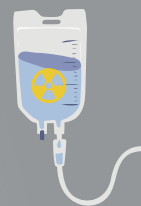
 [www.nmpai.org.in](http://www.nmpai.org.in) | [www.cnmst.org](http://www.cnmst.org)

 [nmpa.newsletter@gmail.com](mailto:nmpa.newsletter@gmail.com)

## Auger Electrons: Opening new realms in therapy

Shweta Rajput

*Department of Nuclear Medicine, AIIMS, New Delhi*



Cancer still remains the leading cause of death worldwide. In India, the estimated number of incident cases of cancer was reported to be 14,61,427 for the year 2022 (crude rate: 100.4 per 1 lakh) [1]. Surgical resection where possible, and external beam radiation therapy (EBRT) remain the favourable treatment options for localised tumors. Chemotherapy, on the other hand, is mainly the feasible option in more aggressive and proliferative tumors with extensive metastasis. However, its efficacy is limited by the serious side effects, normal tissue toxicity, tumor type, and administered dose. Hence, it is very crucial to hunt for the new and more effective therapy options which specifically target the tumor cells sparing the normal tissues.

There are lots of studies being conducted in the development of new approaches to find the treatment options with high therapeutic index. Targeted radionuclide therapy (TRT) is found to be the most promising among those, wherein, specifically the cancer cells are killed by the radionuclides which are successfully conjugated with the biological vectors (peptides, monoclonal antibodies etc). The ability of these radioactive biological vectors to recognise and attach to their binding sites on the tumor cell is attributed for the efficient targeted approach of this therapy. Usually the radionuclides used are alpha (Ac-225, Bi-213, At-211) or Beta (Lu-177, I-131, Re-188) emitting radioisotopes. Beta emitters have the range of several hundred cells in length and thus not suitable for small clusters of cells. Furthermore, the administered activity is limited by the crossfire irradiation of hematopoietic stem cells in the bone marrow which ultimately influence the efficacy of TRT [2]. Alpha particles cause lethal double strand DNA breakage due to their high linear energy transfer (100keV/ $\mu\text{m}$ ) and short range (40-100 $\mu\text{m}$ ) and hence results in high radiotoxicity even in hypoxic tumors. But unfortunately, the full potential of alpha emitters could not be explored due to crisis in their availability and limited number of clinical trials. The global supplies of the most popular alpha emitter (Ac-225) are presently not sufficient to meet the anticipated clinical demand [3]. The candidates that can successfully overcome all these logistic and other issues related to alpha emitters while still providing the similar high LET component for therapeutic application are the Auger emitters. Common examples include I-125, Pt-193m, In-111, Ga-67.

Auger electrons (AEs) are emitted by the radionuclides which decay by electron capture or internal conversion. The electronic transitions in the vacant shells are accompanied by the characteristic x-rays or cascades of auger electrons. These auger electrons deposit huge amount of energy over very short range (nm to  $\mu\text{m}$ ) in biological tissue close to their decay site (Figure-1). Hence, radiation dose is delivered precisely not only to the desired target cell but even more specifically to the sensitive organelles. The potential of auger electrons can be fully explored when these auger emitters can be incorporated into DNA (e.g., 125I-IUdR). This is because the double strand DNA helix has a diameter of 2nm and in a typical auger radiation decay, the highest radiation deposition occurs within spheres of 1-2 nm [4].

This ensures less toxicity to normal cells. Interestingly, due to less reported toxicity in auger therapy, it is possible to inject about ten-fold greater radioactivity of auger emitters than beta emitters. Typically, 5 to more than 35 auger electrons are emitted per decay with energy between a few eV to around 1 keV. Their LET ranges from 4 keV/ $\mu\text{m}$  to 26 keV/ $\mu\text{m}$ . Moreover, their sufficient availability in a non-carrier added form is the added advantage. Low auto-radiolysis (even at high specific activity) of auger emitter labelled radiopharmaceutical offers substantial benefit [5]. Auto-radiolysis is the most serious complication when labelling with alpha emitters is done, which in turn, questions the stability of the labelled compound. Therefore, several factors have to be taken into consideration while doing labeling for auger therapy such as energy of the emitted electrons, half-life of the radionuclide, ratio of emitted photons to electrons, possibility of easy binding to the molecule etc. These auger emitters could be successfully attached to DTPA, DOTA, NOTA, sulfur ligands etc. The radiolabeling method usually employs radio-iodination or radio-metal chelation. However, their specific activity is substantially low when labelled with monoclonal antibodies for therapeutic application.

Some studies have come up with nanostructure-based delivery systems to increase the specific activity and hence optimize the therapeutic efficacy. Nano-medicine is one of the fastest growing scientific fields in the design of new diagnostic and therapeutic methods [2]. The clinical studies of AEs for cancer treatment are limited but encouraging results were obtained in early studies using In-111-DTPA-octreotide and I-125-IUdR, in which tumor remissions were achieved in several patients. The study demonstrated minimal normal tissue toxicity with administered dose as well as promising improvements in the survival of glioblastoma patients with I-125-mAb425 [6]. In another study, I-123-MAPi was found to be a viable agent for the systemic administration and treatment of p53 mutant cancers with significant minimal off-site toxicity in mouse models [7].

Initially the therapeutic potential of auger electrons was ignored due to their low energy and short range. But the whole perception took a turn when the extreme cytotoxic effect of these was observed especially when incorporated into DNA of the nucleus. In the situation of DNA associated decay, the relative biological effectiveness (RBE) of auger electrons is very similar to alpha particles. Besides DNA, the cell membrane and mitochondria could also serve as the critical targets for these AEs. Hence, auger therapy harbours tremendous potential in the domain of targeted radionuclide therapy in the near future. It has opened avenues for a novel therapeutic option. The contribution of Pierre Auger truly holds much more promising applications which the scientists in this field envision.

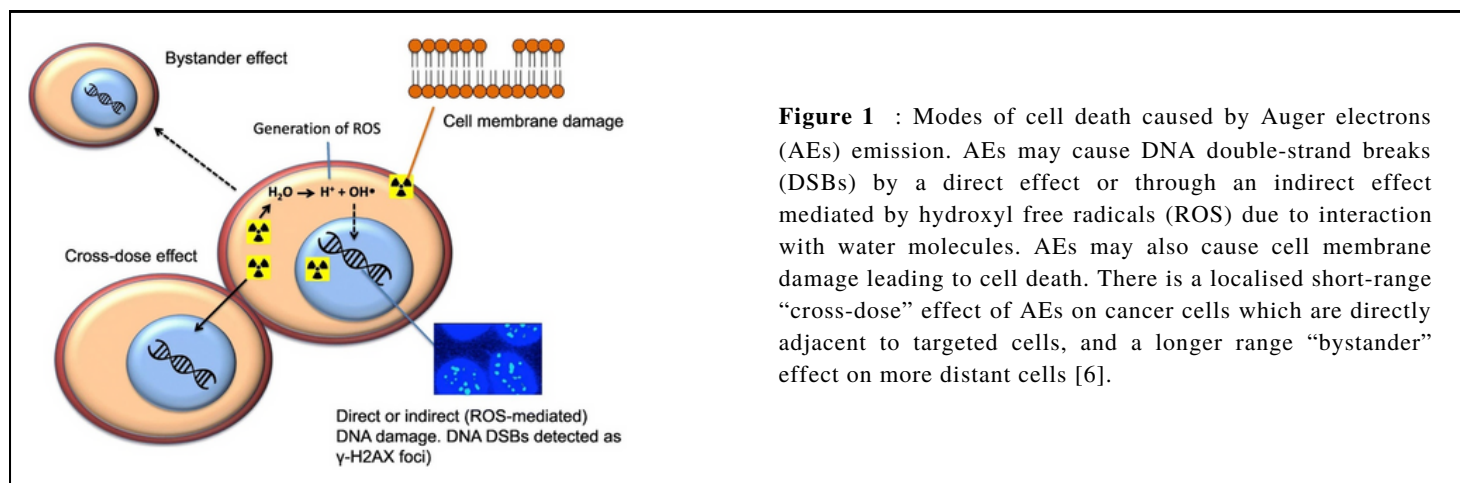
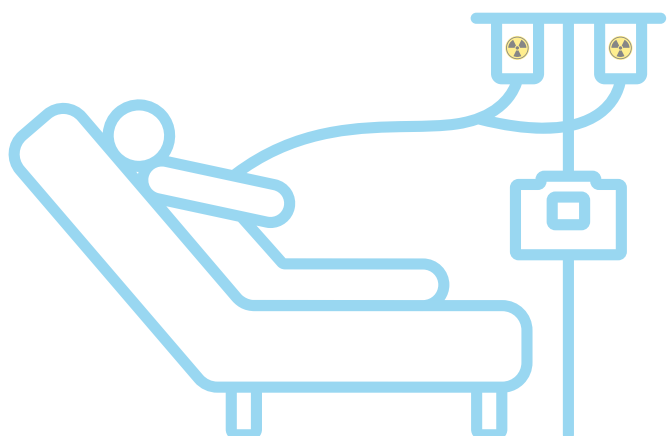


**Figure 1** : Modes of cell death caused by Auger electrons (AEs) emission. AEs may cause DNA double-strand breaks (DSBs) by a direct effect or through an indirect effect mediated by hydroxyl free radicals (ROS) due to interaction with water molecules. AEs may also cause cell membrane damage leading to cell death. There is a localised short-range “cross-dose” effect of AEs on cancer cells which are directly adjacent to targeted cells, and a longer range “bystander” effect on more distant cells [6].

## REFERENCES

1. Sathishkumar K, Chaturvedi M, Das P, Stephen S, Mathur P. Cancer incidence estimates for 2022 & projection for 2025: Result from National Cancer Registry Programme, India. *Indian J Med Res.* 2022. doi: 10.4103/ijmr.ijmr\_1821\_22.
2. Gharibkandi NA, Gierałtowska J, Wawrowicz K, Bilewicz A. Nanostructures as radionuclide carriers in auger electron therapy. *Materials.* 2022;15(3):1143.
3. Engle JW. The production of Ac-225. *CurrRadiopharm.* 2018;11(3):173-179.
4. Buchegger F, Perillo-Adamer F, Dupertuis YM, Bischof Delaloye A. Auger radiation targeted into DNA: a therapy perspective. *Eur J Nucl Med Mol Imaging.* 2006;33:1352-1363.
5. Aghevlian S, Boyle AJ, Reilly RM. Radioimmunotherapy of cancer with high linear energy transfer (LET) radiation delivered by radionuclides emitting  $\alpha$ -particles or Auger electrons. *Adv. Drug Deliv Rev.* 2017;109:102-118.
6. Ku A, Facca VJ, Cai Z, Reilly RM. Auger electrons for cancer therapy—a review. *EJNMMI radiopharmchem.* 2019;4:1-36.
7. Wilson T, Pirovano G, Xiao G, Samuels Z, Roberts S, Viray T, et al. Parp-targeted auger therapy in p53 mutant colon cancer xenograft mouse models. *Mol Pharm.* 2021;18:3418-3428.



# TIME-OF-FLIGHT IN PET: PRINCIPAL, HISTORY, AND RECENT ADVANCES IN CRYSTAL TECHNOLOGY

Abdul Shaikh\*, Viraj Sawant\*, Rakhee Vatsa, Venkatesh Rangarajan

*Department of Nuclear Medicine and Molecular Imaging*

*Advanced Centre for Treatment Research and Education in Cancer, Tata Memorial Care*

\*Both share equal contribution



## INTRODUCTION

Positron emission tomography (PET) is an advanced imaging modality based on the coincidence imaging of annihilated photons. The signal is produced when the positron emitted by the decay of an unstable radionuclide (e.g., fluorine-18 [F-18], gallium-68 [Ga-68]) combines with an electron in the vicinity and undergoes annihilation. During the annihilation process, two 511 keV coincident photons are emitted (Figure 1). These photons are deflected at an angle of  $180^\circ \pm 0.25^\circ$  and travel toward the surrounding detector in the provided field of view (FOV) along the line of response (LOR), giving a time coincidence [1].

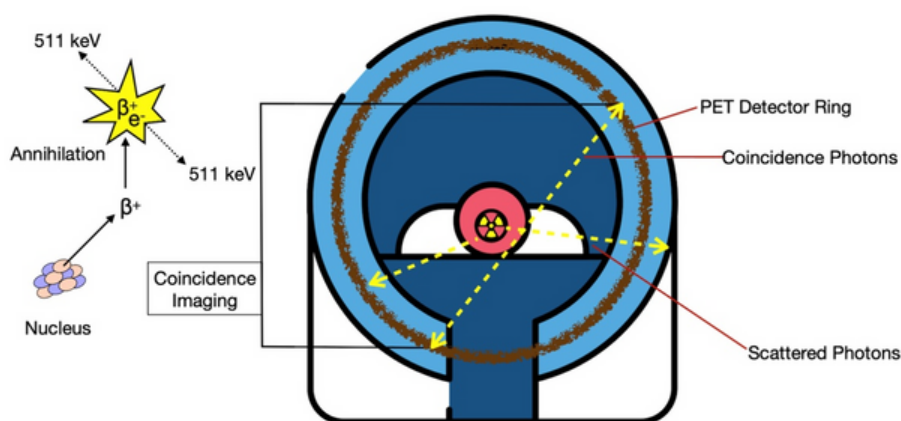


**Figure 1** : Schematic diagram showing annihilation and coincidence imaging

This technique has no impact on spatial resolution but significantly reduces the statistical noise in reconstructed images, which is a major limitation of PET. Using time-of-flight (TOF) PET, the event's location along the LOR can be determined more precisely because of the system timing resolution [2,3]. Ideally, if the system timing resolution provides a spatial uncertainty  $\Delta x$  ( $\Delta x = c \cdot \Delta t/2$ , where  $c$  is the speed of light in vacuum) along the LOR that is comparable to or better than the spatial detector resolution, then image reconstruction can essentially be described as placing events directly in the most likely image voxels. For an average detector with a spatial resolution of 4.5 mm, the system timing resolution translates to 30 ps, which is at least an order of magnitude better than that currently achieved in commercial PET systems.

## HISTORY OF TIME-OF-FLIGHT PET

In the 1980s, several TOF PET modalities were constructed using barium fluoride (BaF<sub>2</sub>) or Cesium fluoride (CsF) as the primary crystal choices. These systems were able to achieve 500 ps time resolution, which provided improvement in statistical noise. However, their performance was restricted by the materials and technology available at that time. Due to the low stopping power of both BaF<sub>2</sub> and CsF scintillators, they had limited spatial resolution and detection effectiveness than bismuth germanate (BGO), which was the choice of PET detector at that time [1,4]. BaF<sub>2</sub> requires quartz window photomultiplier tubes because of UV emission spectra, whereas CsF is hygroscopic with poor light output and energy resolution and incompatible with block detector technology [4].

Furthermore, TOF PET scanners depend on using additional electronics to do time-of-flight measurements, and such electronics fail to provide good results. With recent advancement in crystal technology and electronics processing, a new generation of TOF PET systems are under development, overcoming the limitations of previous systems.

## RECENT ADVANCES

The development of lutetium oxyorthosilicate (LSO or  $\text{Lu}_2\text{SiO}_5:\text{Ce}$ ) gives a major breakthrough in the modern TOF PET system [5]. The crystal has a similar attenuation range as BGO but with faster decay time and high light output yield. Several materials have a similar chemical composition and scintillation properties as LSO, such as mixed lutetium silicate (MLS), lutetium gadolinium oxyorthosilicate (LGSO), lutetium-yttrium oxyorthosilicate (LYSO), and lutetium fine silicate (LFS). With a coincidence timing resolution of 600 ps, Philips first released LYSO-based pet camera in 2006 [6,7].

A recently developed lanthanum bromide doped with a 5% cerium crystals detector module has been reported to achieve 310-350 ps full-width half maximum (FWHM) coincidence timing resolution with both LYSO and  $\text{LaBr}_3:5\%\text{Ce}$  cameras [8]. Significant improvement in performance in comparison to other scanners is observed experimentally. Some newly discovered materials are quite promising for TOF PET. These materials are  $\text{LaBr}_3:\text{Ce}$  with cerium concentrations other than 5%,  $\text{CeBr}_3$ , and  $\text{LuI}_3:\text{Ce}$ . These new scintillator materials are truly astounding. All of them have a light output of at least 150% that of  $\text{NaI:Tl}$ , energy resolution (at 662 keV) that is better than 4% FWHM, and timing resolution that is better than barium fluoride.  $\text{LaBr}_3:30\%\text{Ce}$  achieves a timing resolution that is a factor of two better than  $\text{BaF}_2$  (69 ps for a single crystal, implying 100 ps, FWHM coincidence timing) [9,10]. However,  $\text{LuI}_3:\text{Ce}$  stands out among these remarkable new materials. It has a light output of 100,000 photons/MeV (2.6 times that of  $\text{NaI:Tl}$ ), energy resolution of 4% FWHM (2.5 times better than LSO), and coincidence timing resolution of 125 ps FWHM (better than  $\text{BaF}_2$ ) [11].

Despite promising new materials, the ideal scintillator has not yet been discovered. TOF PET would benefit enormously from new scintillators that combine high light output and short decay time (for excellent timing resolution), high density, effective atomic number (for better spatial resolution and efficiency), and good linearity (for excellent energy resolution).

Significant activities related to TOF hardware technology have been observed in the last few years. Special interest has been noted in photo-sensor development in third-generation systems leading to the commercial introduction of silicon photomultiplier (SiPM) based digital whole body TOF PET system [12]. A long axial length and improved spatial resolution make these new systems much better at TOF resolution and sensitivity than their predecessors [13]. The TOF resolution is directly related to the coincidence timing resolution CTR of the PET scintillation detector, which is a function of the type of photosensor and the design of the detector [13]. A detector CTR is determined by a number of scintillations, types of photo-sensors, detector design, and electronics. The calibrations and variability of detector performance also define the system TOF. It can potentially improve diagnostic performance and further reduce imaging times to less than ten minutes for a whole-body scan with the latest digital TOF PET system. [14,15].



In recent years, many major vendors have switched to a digital (SiPM-based) system, which has generally improved the field of view in the axial direction. As a result of minimal or no multiplexing, the TOF resolutions of these scanners range from 214 to 380 ps [13], while the dead time is very low compared to traditional PMT-based systems. Differences in TOF resolution are primarily driven by the choice of scintillation SiPM array and detector design in signal multiplexing and light collection efficiency.

TOF helps to improve the reconstruction consistency by providing additional information on the particle's trajectory, which can better estimate the particle's energy [16]. This, in turn, reduces the need for corrections, which can be a source of inconsistency. As a result of intrinsic isotope decay fraction in various isotopes, the emission properties and contaminating coincidences occur more frequently. These isotopes will also benefit from TOF technology with a higher SNR for the same number of counts. This also reduces scatter and random photons detection as an additional benefit [17]. As the current best possible TOF time resolution system has a 200 ps timing resolution but does not define the accurate source location, reconstruction with all its contaminant limitations is still required [18]. With the advancement of technology, time resolution has also been improved so that the radiation events have entered a new era of TOF where they can be directly localized without the use of the reconstruction process, termed direct positron emission tomography (DPET). This is similar to an ultrasound where TOF difference is also considered, i.e., speed of sound in tissue for tissue depth reflection. The research is going on in the DPET field; the use of the Cherenkov luminance mechanism has also been reported to achieve fast timing signals and the CNN network to predict the timing information [19]. These integrations between the Cherenkov radiation directly and the photo-sensor optimize the light transport and photon detection properties.

In the future, TOF should be able to acquire images with high SNR at low radiation doses and short acquisition time once larger-scale systems with more efficient detectors are developed [20]. Also, with the development of critical technologies, acquisition hardware and software, real-time imaging in TOF is possible where no reconstruction step is involved giving real-time images as they are acquired.

## REFERENCES

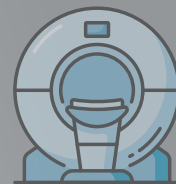
1. DiFilippo FP. Instrumentation and Principles of Imaging: PET. In: Carli MF, Lipton MJ editors. Cardiac PET and PET/CT Imaging. Springer New York, NY; 2007.p.3–18.
2. Budinger TF, Derenzo SE, Huesman RH, Jagust WJ, Valk PE. High-resolution PET (positron emission tomography) for Medical Science Studies. 1989; United States: N.p., 1989. Web. doi:10.2172/5473405.
3. Schaart DR. Physics and technology of time-of-flight PET detectors. *Phys Med Biol*. 2021; 66:1361-6560.
4. Yu X, Zhang X, Zhang H, Peng H, Ren Q, Xu J, et al. Requirements of Scintillation Crystals with the Development of PET Scanners. *Crystals*. 2022; 12:1302. <https://doi.org/10.3390/cryst12091302>.
5. Lecoq P, Auffray E, Brunner S, Hillemanns H, Jarron P, Knapitsch A, et al. Factors Influencing Time Resolution of Scintillators and Ways to Improve Them. *IEEE Trans Nucl Sci*, 2010; 57:2411-2416.

6. Surti S, Kuhn A, Werner ME, Perkins AE, Kolthammer J, Karp JS. Performance of Philips Gemini TF PET/CT scanner with special consideration for its time-of-flight imaging capabilities. *J Nucl Med.* 2007; 48:471–480.
7. Moses WW, Ullisch M. Factors influencing timing resolution in a commercial LSO PET camera. *IEEE Trans Nucl Sci.* 2006; NS-53:1–8.
8. Kuhn A, Surti S, Karp J, Muehllehner G, Newcomer F, VanBerg R. Performance Assessment of Pixelated LaBr<sub>3</sub> Detector Modules for TOF PET. *IEEE Trans Nucl Sci.* 2006; 53:1090-1095.
9. Schaart DR. Physics and technology of time-of-flight pet detectors. *Phys Med Biol.* 2021; 66:09TR01.
10. Moszynski M, Kapusta M, Nassalski A, Szczesniak T, Wolski D, et al. New prospects for time-of-flight PET with LSO scintillators. In: Yu B, editor. *Proceedings of The IEEE 2005 Nuclear Science Symposium*; San Juan, Puerto Rico. 2005;J3–18.
11. Kuhn A, Surti S, Karp JS, Raby PS, Shah KS, et al. Design of a lanthanum bromide detector for time-of-flight PET. *IEEE Trans Nucl Sci.* 2004; NS-51:2550–2557.
12. Nemallapudi MV, Gundacker S, Lecoq P, Auffray PE. Single photon time resolution of state of the art SiPMs. *J Inst.* 2016; 11:10016-10016.
13. Surti S, Karp JS. Update on latest advances in time-of-flight PET. *Phys Med.* 2020; 80:251-258.
14. Berg E, Cherry SR. Using convolutional neural networks to estimate time-of-flight from PET detector waveforms. *Phys Med Biol.* 2018; 63:02LT01.
15. Korpar S, Dolenc R, Križan P, Pestotnik R, Stanovnik A. Study of TOF PET using Cherenkov light. *Nucl Instrum Methods Phys Res.* 2011; 654:532-538.
16. Moszynski M, Ludziejewski T, Wolski D, Klamra W, Avdejcikov VV. Timing properties of GSO, LSO and other Ce doped scintillators. *Nucl Instr Meth.* 1996; 372:51–58.
17. Vandenberghe S. Recent developments in time-of-flight pet. *Physica Medica.* 2018; 52:69.
18. Lamprou E, Benlloch JM. Exploring TOF capabilities of PET detector blocks based on large monolithic crystals and analog SiPMs. *Physica Medica.* 2020; 70:10–18.
19. Cerenkov PA. Visible radiation produced by electrons moving in a medium with velocities exceeding that of light. *Phys Rev.* 1937; 52:378-379.
20. Kwon SI, Ota R, Berg E, Hashimoto F, Nakajima K, Ogawa I, et al. Ultrafast timing enables reconstruction-free positron emission imaging. *Nat Photonics.* 2021; 15:914-918.

## SCINTILLATION DETECTORS IN NUCLEAR MEDICINE: EVOLUTION AND ADVANCEMENTS

Aryan Kumar, Naresh Kumar, Shweta Rajput, Priyanka Gupta

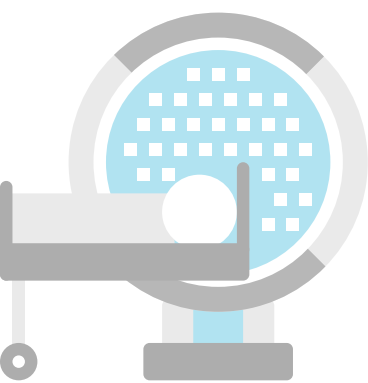
*Department of Nuclear Medicine, AIIMS, New Delhi*



Scintillators, the sensors for ionizing radiation, serve as the heart of the detection systems in Nuclear Medicine. ZnS screen was the first scintillator device made by Sir William Crookes in 1903, and their scintillations were measured using a spintharoscope. Scintillators got attention in 1944 when Curran and Baker replaced the naked eye measurement with the newly developed PMT [1, 2]. With the advent of time, the potential of scintillators as robust ionizing radiation detectors was explored and established. High density, high atomic number, high light output and conversion efficiency, linear conversion, short decay time, optimum refractive index, an appropriate wavelength of emitted light, and good mechanical stability were some of the parameters attributed to their widespread applications in both imaging as well as counting systems.

There are many phases in developing scintillation detectors (Figure 1). The first phase was the early use of ZnS, CaWO<sub>4</sub>, and barium platinocyanide screens as scintillators by Röntgen, Crookes, Rutherford, and many others [4]. Photomultiplier tubes' introduction in the 1940s and the discovery of the NaI (Tl) and CsI (Tl) scintillators at the beginning of the 1950s triggered the second phase [4-7]. In the third phase, rare earth materials (REE) and crystals with high-melting-point materials were used as luminescence centers. The use of REE elements (mainly Ce and Eu) as dopants in various materials developed heavily during the fourth phase, and many lanthanide-activated halides were discovered. The co-doping technique and dedicated band gap engineering improved multiple properties of existing scintillation materials. The advancement in manufacturing technologies brought forward garnet compounds and ceramic scintillators [4].

Currently, we are in the fifth phase of the development of scintillators. It requires a deeper understanding of the scintillation processes to make the necessary modifications and advancements to match the current impetus in imaging sciences. Energy resolution improvement has emerged as the most challenging task among the present demands. Scintillating materials with fast decay of their luminescence are in second and utmost demand.





These scintillators were observed to be more sensitive to photon events, enabling high-sensitivity gamma imaging without mechanical collimation. The average detection sensitivity in the field of view (FOV) was 300 cps/MBq. According to the point source imaging study, the proposed gamma camera can accurately locate a point source with 100  $\mu$ Ci Tc-99m total activity with 1 s measurement time. For a 300  $\mu$ Ci 99mTc point source, the average positioning accuracy was  $4.8 \pm 2.0$  mm,  $6.2 \pm 2.8$  mm and  $7.4 \pm 4.2$  mm with 10 s, 3 s, and 1 s measurement time, respectively. These scintillators could clearly resolve four 300  $\mu$ Ci point sources with 1s acquisition time. With the fusion of gamma activity distribution and optical image, the gamma camera has been noted to be much more suitable for practical medical applications such as surgical guidance [10].

The system consisting of four detectors arranged around the organs-on-chips (OOC) device, a micro-device mimicking in-vivo organs, finds expanding uses in drug discovery and disease modelling. Each detector comprises two monolithic Lutetium–yttrium oxy orthosilicate (LYSO) crystals covered with silicon photomultipliers (SiPMs) on multiple surfaces. Clement et al. reported the application of Monte-Carlo simulation (MCS) trained convolutional neural network (CNN) for predicting the first gamma-ray interaction position in the detector from the light patterns that the SiPMs on the surfaces of the detector recorded. With the line of responses (LORs) developed by the predicted interaction positions, the simultaneous algebraic reconstruction technique (SART) has been rebuilt. After reconstruction, the mean spatial resolution of the image was 0.53 mm [11]. With the system made of multiple monolithic LYSO crystals, 0.5 mm spatial resolution in PET is achievable by directly predicting the scintillation position from light patterns created with SiPMs.

Scintillation detectors based on new photosensors are upcoming candidates that meet the requirements much better, and focusing on their further development is in high demand [12, 13]. The latest SiPM generations are adequate sensor element replacements of PMT in scintillation detectors. The gamma-ray detection performance of scintillation detectors based on SiPM has been reported in various studies. The main requirements for SiPM are high pixel density and photon detection efficiency (PDE), which play a vital role in the linearity and energy resolution of the entire detector [14-17]

The use of scintillating ion exchange resins has facilitated the extraction and counting of minimal activities of beta-emitting isotopes in the form of ions in large volumes of water (i.e. cooling water, effluents, rain, rivers, etc.), avoiding the inconvenience of large-scale concentration by evaporation. The cationic-type resin consists of plastic scintillator spheres with sulfonated surfaces. These resins are suitable for detecting radioisotopes like S-90 and Ca-45. The surfaces of the anionic type of plastic scintillating spheres are made of a quaternary ammonium compound for absorption of such activities as  $^{14}\text{CO}_2$  and  $^{32}\text{PO}_4$  [18-20].

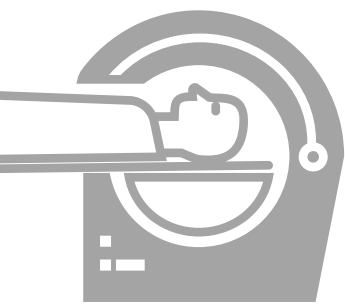
Alpha detection proves to be the most cumbersome process. A new tool, an optical fiber-based alpha particle detector, could directly detect alpha particles in the subject. For 5.5MeV alpha particles, the count rate was around two times higher, and the pulse heights were about five times higher using the ZnS(Ag) fiber detector in contrast with those using the LYSO(Ce) fiber detector. For the maximum energy of 2.28 MeV beta particles and 0.66 MeV gamma photons, the ZnS(Ag) fiber detector produced zero counts, but it yielded small counts from natural alpha particles. ZnS(Ag) fiber detector was insensitive to beta particles and gamma photons and could only selectively detect alpha particles. [21].

Several advances have been made to understand the mechanisms that drive the scintillator performance. However, these advances have largely yet to be translated to commercial products due to the many barriers in the transition from discovery to production. Some issues that typically limit the scaling of materials are related to complex synthesis, poor consistency in performance, and an unacceptable production cost, which are important factors for large-scale deployment. Researching scintillating materials has been a continuous effort for the last decades. The evolution in the scintillating materials is a multidisciplinary approach requiring simultaneous advancements in photodetectors, signal processing, and computing or data flow capacity. The material science when complexed with better electronics and computing systems could be a big boost in image detection.

## REFERENCES

1. Leo WR. *Techniques for Nuclear and Particle Physics Experiments* (2nd ed.). Springer. 1994. doi:10.1007/978-3-642-57920-2.
2. Dyer SA. *Survey of Instrumentation and Measurement*. Wiley-Blackwell. 2001. ISBN 978-0471394846.
3. Dujardin C, Auffray E, Bourret-Courchesne E, Dorenbos P, Lecoq P, Nikl M. et al. Needs, Trends, and Advances in Inorganic Scintillators. *IEEE Trans Nucl Sci*. 2018; 65:1977-1997.
4. Ljungberg M, ed. *Handbook of Nuclear Medicine and Molecular Imaging for Physicists, Instrumentation and Imaging Procedures, Volume I*.
5. Hofstadter R. Alkali Halide Scintillation Counters. *Phys Rev*. 1948; 74, 100-101.
6. Hofstadter R. The Detection of Gamma- Rays with Thallium- Activated Sodium Iodide Crystals. *Phy Rev*.1949; 75:796-810.
7. Sciver WV, Hofstadter R. Scintillations in Thallium-Activated CaI<sub>2</sub> and CsI. *Phy Rev*. 1951; 84:1062-1063.
8. Saleh L, Paul Vaska P. Performance of a Monolithic Crystal PET Detector with Integrated Retroreflectors. *J Nucl Med*. 2022; 63:3314.
9. Lee D, Cherry S, Kwon SI. Colored reflectors to improve timing resolution of BGO-based time-of-flight PET detectors. *J Nucl Med*. 2022; 63:2342.
10. Hu Y, Liu L, Lyu Z, Zhang D, Xu T, Qi C, et al. A high-sensitivity hand-held medical gamma camera with mosaic-patterned scintillation detector. *J Nucl Med*. 2022; 63:2339.
11. Clement C, Birindelli G, Pizzichemi M, Pagano F, Julio MKD, Ziegler S, et al. Concept Development of an On-Chip PET System. *J Nucl Med*. 2022; 63:3237.
12. Sadigov A, Ahmadov F, Ahmadov G, et al. A new detector concept for silicon photomultipliers. *NuclInstrum Methods A*. 2016; 824:135.

13. Holik M, Ahmadov F, Ahmadov G, Akbarov R, Berikov D, Mora Y, et al. Miniaturized read-out interface “Spectrig MAPD” dedicated for silicon photomultipliers. *NuclInstrum Methods A*. 2020; 978:164440.
14. Ahmadov F, Ahmadov G, Akbarov R, Aktag A, Budaket E, Doganci E, et al. Investigation of parameters of new MAPD-3NM silicon photomultipliers. *J Instrum*. 2022;17:C01001.
15. Marques L, Vale A, Vaz P. State-of-the-art mobile radiation detection systems for different scenarios. *Sensors*. 2021; 21:1051.
16. Ahmadov F, Ahmadov G, Guliyev E, Madatov R, Sadigov A, Sadygov Z, et al. New gamma detector modules based on micropixel avalanche photodiode. *J Instrum*. 2017;12:C01003.
17. Ahmadov G, Ahmadov F, Holik M, Berikov D, Sadygov Z, Akbarov R, et al. Gamma-ray spectroscopy with MAPD array in the readout of LaBr<sub>3</sub>:Ce scintillator. *J Instrum*. 2021;16:P07020.
18. A. H. Heimbuch and H. Y. Gee, USAEC Report no. NYO9138 (1962)
19. A.H. Heimbuch et al., USAEC Report no. NYO-10405 (1964)
20. Nicoll DR, Routley REU. Proc Symposium Paris. *Electronique nucléaire* (1963) p.79.
21. Yamamoto S, Aoki I, Higashi T. Optical fiber-based ZnS(Ag) detector for selectively detecting alpha particles. *ApplRadiatIsot*. 2021;169:109495.



## Radiation Protection of Auxiliary staff in Nuclear Medicine Department



Indira V Upadhya

Department of Nuclear Medicine, Cytecure Cancer Hospital, Yelahanka, Bengaluru

Radiation protection is an utmost requirement while working with radioactive sources. It is based on the principles of ALARA (as low as reasonably achievable), that is, using the golden rules of radiation safety: minimum time, maximum distance, and optimum shielding. The core members of the team working in any nuclear medicine department are nuclear medicine physician and nuclear medicine technologist(s). One of these core team members, generally take up the role of “Radiation Safety Officer” too. The auxiliary staff are those supporting team mates who play significant roles for the departmental workflow. They will never directly handle radioactivity. However, the possibility of their encounter with radioactive patients cannot be avoided.

The auxiliary staff can be any of the following types:

- Staff recruited at reception and billing
- Housekeeping / Scavenger Staff
- Patient Care Staff
- Nursing Staff

The common rule for every staff is to try and complete the conversation and instructions before administration of radioactivity to the patient. If any additional communication is required, the patient attender, whenever available, should be opted to convey the messages, who is generally eager and more than happy to be involved in the management of his relative’s treatment.

Restricted entry to the radiation area (radiopharmacy, radioactive patient waiting, imaging and therapy rooms), preferably guarded by security staff for monitoring can reduce the unnecessary entry of the auxiliary staff to such areas.

The transport of radioactivity and the radioactive patient should be minimized by planning the work protocol and areas, in such a way that this rule can be implemented. The transport, whenever necessary, should be conducted with proper precautions, identified radiation symbols on the shield used for transport, avoiding heavily occupied areas.

### Staff at Reception and Billing

All the formalities of documentation and payment should be completed in the beginning and the staff should avoid entering the access-controlled area, unless and until, it is absolutely necessary. In cases where female staff are of reproductive age group, the identified pregnancy should be declared at the earliest and alternative arrangement of service in the hospital should be planned.



Radiation source, that arrives at the department, should NEVER be kept at the reception. It is to be received by the authorized core team member in the control area and transferred to the prescribed area.

The staff should be periodically trained or made aware of the basic radiation safety rules and the identified radiation symbols. This practice will prevent them from unnecessary panic, anxiety or fear and they can perform efficiently and peacefully. A sense of radiation safety culture should be developed among the staff to maintain minimum exposure of self from unwanted exposure to the radioactive patient or radioactivity in the control area (although shielded).

The radioactive patients should be provided a waiting area, inside the access-controlled area to avoid undue exposure to the reception and billing staff. In case of any unresolved issue or enquiry with a radioactive patient, should be directed to the concerned authorized personnel, without wasting any time. This gives an impression of efficient use of time as well as radiation safety for the auxiliary staff.

The stationery items required in the reception and billing area should not be stored in the access-controlled area.

#### Housekeeping / Scavenger Staff

The paediatric cases and the patients without urine control should be instructed to wear diapers to avoid urine spillage. In case of urine spillage, it needs to be managed by the appropriately trained housekeeping staff.

The cleanup of the washroom or any other maintenance work should be checked daily morning before the patients are administered with radioactivity. In case of any need of intermittent cleaning, the housekeeping staff should do so, only after the radioactive patients are requested to be seated at a maximum possible distance, preferably behind a thick wall, till the cleaning work is completed.

In case of High Dose Therapy (HDT) isolation wards, the rooms should be taken up for cleaning by giving maximum possible delay time after the discharge of the patients, or just before the next admission is being scheduled. The HDT patients should be educated and encouraged, not to waste any food material and if they still generate any, dispose the waste generated by them, especially the leftover food in specially assigned lead lined dustbin, so that this work can be avoided by the house keeping staff, when they come for cleaning.

There should be a poster of spill management with self-explanatory pictures for the housekeeping staff to easily follow during the actual spill management under supervision, along with pre- and post-cleaning measurements of the radioactivity by the RSO. The house keeping staff should be rotated and care should be taken that a single staff is not performing the task constantly.

#### Nursing Staff

This section is bound to handle radioactive patients; however, a secure and patent IV line makes the flow of nuclear medicine procedures very easy. This step should be performed very carefully to avoid extravasation at later stage and to re-secure the IV line for a radioactive patient. The nurses should use gloves when the IV line is being removed before release of the patient.

All the activities like history taking, informed consent, rapport building for patient cooperation and educating the patient of the radioactivity, restriction of the staff to provide physical support should also be conveyed before administration of the radioactivity. In cases of emergency handling of radioactive patients, the nurse should first inform the concerned physician and plan well, without panic or anxiety, before actually handling the patient. The expert team that will handle the emergency should be contacted and brought to the spot as soon as possible to give best service and improve the benefit risk ratio for all.

A double injector (with saline and contrast syringes) should be present in the positron emission tomography-computed tomography (PET-CT) acquisition room, which administers saline pre- and post-contrast injection. It prevents the need of nursing staff to be proximal to radioactive patient and taking risk of being in a CT room just before the start of CT scan.

The radioactive patients in the waiting area can be monitored by the nursing staff through the CCTV monitor, which serves the dual purpose of radiation safety and patient care.

Overall, Radiation Protection for the staff in a nuclear medicine department can be successfully implemented by:

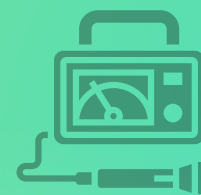
- Judicious and optimum use of radioactivity, procuring minimum that is required,
- Handling of radioactivity with proper safety precautions by authorized personnel only
- Avoiding any careless disposal of radioactive waste.



## Radiation Surveillance at the Delay Tanks Facility: An Institutional Experience

Amandeep Kaur, Yasmeen Atwal Sonik, Bhavay Sonik

Department of Nuclear Medicine, Guru Gobind Singh Medical College and Hospital, Faridkot, Punjab.

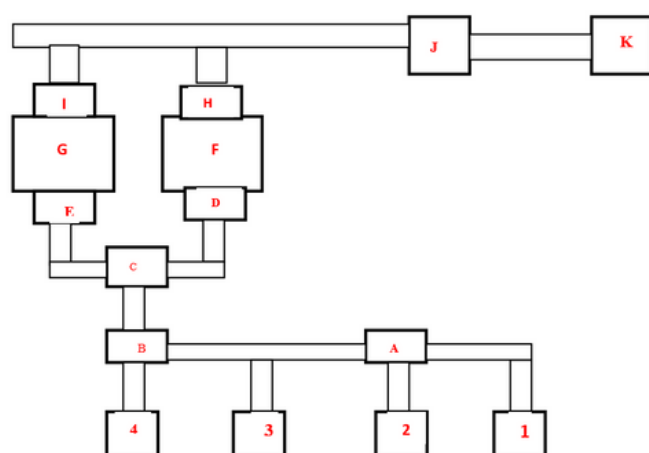


Guru Gobind Singh Medical College & Hospital (GGSMC&H), under Baba Farid University of Health Sciences (BFUHS), Faridkot, Punjab; houses the sole government aided Nuclear Medicine Department of Punjab. This department, built in accordance with Atomic Energy Regulatory Board (AERB) specifications, has a high dose iodine therapy (HDIT) unit apart from dedicated positron emission tomography/computed tomography (PET/CT) and single photon emission computed tomography (SPECT) camera facilities, which cater primarily to the huge population of the Malwa belt of Punjab with secondary referral from the rest of the state.

The HDIT unit is located on the first floor of the three-floor facility and has four isolation rooms. In accordance with AERB regulations, the HDIT unit have a separate sewerage draining system from the rest of the department. The layout is such that the sewerage from HDIT rooms is drained into two twin concrete delay tanks of 3x2x2 meters each with a capacity of 12000 L (Figure 1). A set of floating switches have been installed at the height of one meter (at 85% of the total fill volume) in both delay tanks to monitor effluent levels, so that they are filled alternately.

The flow to the delay tanks is regulated by 11 gate valves, which are manually operable and are thus also a site of potential radiation leakage if any were to occur. The current study took this aspect of potential radiation leakage into account, and a radiation survey was carried out around the delay tank facility for 16 consecutive weeks using a Geiger-Müller based radiation detector (RAM GENE-1, ROTEM) to rule out any potential radiation leakage hazards, more specifically at these 11 gate valve locations (Figure 1).

During the 16-week study period, 27 patients were given HDIT, of whom 7 were male and 14 were female. The administered dose of radioiodine (I-131) was in the range of 80–245 mCi (mean 162.5 mCi). The average stay in isolation was 2-4 days until the permissible radiation exposure rate of less than 5 mR/hr at a 1-meter distance from the patient was reached.



| Locations | Demarcation  |
|-----------|--|
| A         | Manhole chamber of 1 <sup>st</sup> and 2 <sup>nd</sup> Isolation rooms   |
| B         | Manhole chamber of 3 <sup>rd</sup> , 4 <sup>th</sup> Isolation rooms (which drain all waste liquid to common gate-valve of all four isolation rooms) |
| C         | Chamber containing common gate valve, which lead the waste liquid of all four isolation rooms to inlet valve chambers of two delay tanks             |
| D         | Chamber for Inlet valve of 1 <sup>st</sup> Delay tank  |
| E         | Chamber for Inlet valve of 2 <sup>nd</sup> Delay tank  |
| F         | 1 <sup>st</sup> Delay tank of 12,000lts capacity   |
| G         | 2 <sup>nd</sup> Delay tank of 12,000lts capacity   |
| H         | Chamber for Outlet valve of 1 <sup>st</sup> delay tank   |
| I         | Chamber for Outlet valve of 2 <sup>nd</sup> Delay tank   |
| J         | Chamber of Inspection point operated with manual valve system  |
| K         | Manhole of Hospital sewerage pipeline  |

Figure 1 : Layout plan of Delay Tank Facility

During the 16-week study period, 27 patients were given HDIT, of whom 7 were male and 14 were female. The administered dose of radioiodine (I-131) was in the range of 80–245 mCi (mean 162.5 mCi). The average stay in isolation was 2-4 days until the permissible radiation exposure rate of less than 5 mR/hr at a 1-meter distance from the patient was reached.

The sewerage from HDIT rooms was diverted, with manually operable gate valves, to fill delay tank 1, as delay tank 2 was already filled to its capacity and was closed for delay and decay to dispose of radioactivity. We observed that radiation exposure at location F of delay tank-1 gradually increased as the tank filled during the study period. On the other hand, the radiation exposure rate at location G of delay tank-2 decreased as the tank was closed for the duration of the study because of the physical decay of I-131 over that time. Further, at locations J and K, there were an almost constant exposure rate, as shown in figure 2 and figure 3.

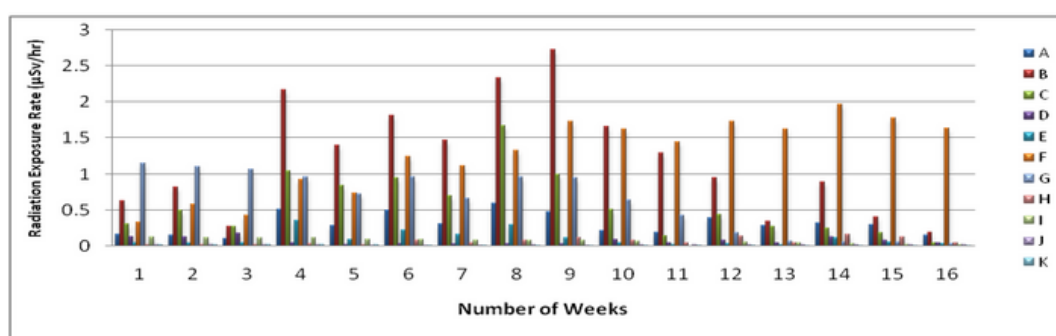


**Figure 2** : Demonstrates the radiation exposure rates recorded over a 16-week study period around the delay tank facility.

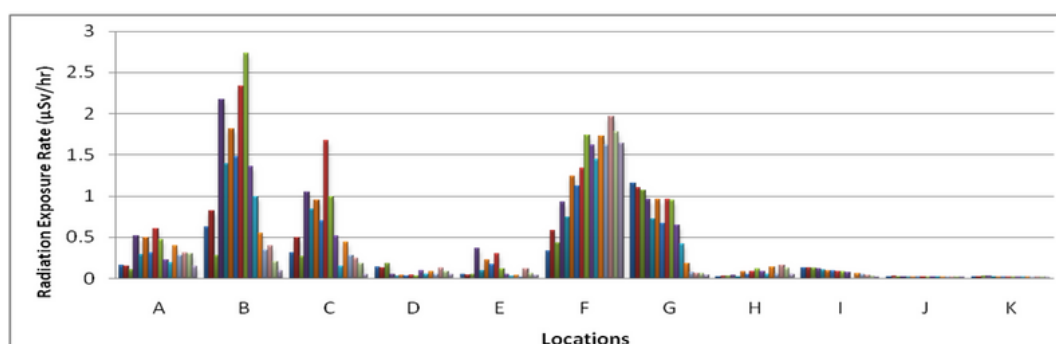


**Figure 3** : Shows the rate of radiation exposure recorded at 11 different locations marked around the delay tank facility from week 1 to week 16.

The highest exposure rate was found at location B, which is a common gate valve that connects the collective sewerage pipes of four isolation rooms via pipeline to common gate valve C. The second highest exposure rate was recorded at location C, which is the common gate valve leading the sewerage waste to both the delay tanks, as shown in Figure 3.

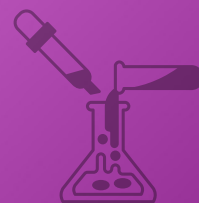
High radiation exposure rates were observed at those locations, which were the primary receiving end of sewerage waste from the isolation rooms, but these rates were found to be well within the permissible limits established by AERB.

From the results of the present study, we would like to stress upon the need of routine radiation survey of potential leakage points of HDIT unit as this is an important component of overall radiation safety in sewerage delay tank facilities, and helps in keeping the radiation exposure to acceptable levels by identifying timely radiation leakage if any, thus, saving from any major radiation leakage exposure in future.

## F-18-FDG: An overview of Radiochemical Identity and Radiochemical purity

Sandeep Kumar Sharma, B N Kar

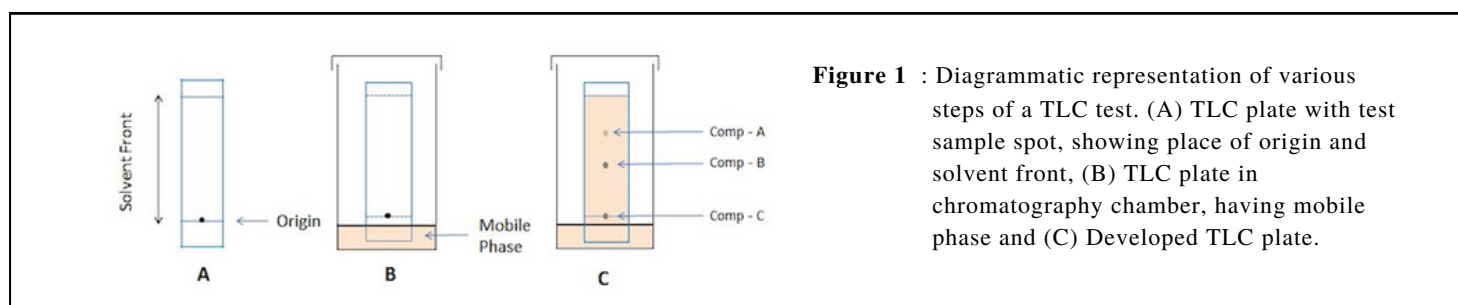
FDI Care- Cyclotron Unit, Futuristic Diagnostic Imaging Pvt. Ltd., Jigani Industrial Area, Bangalore- 560105



F-18-FDG (fluorodeoxyglucose) is the most widely used positron emission tomography (PET) radiopharmaceutical. Primarily, it is used in the detection and staging of various kinds of cancer. The use of F-18-FDG increased due to its broad spectrum of applications. Production of F-18-FDG is a multi-step procedure that involves production of F-18-Fluoride in a cyclotron by bombarding O-18 enriched water with a proton beam, trapping of F-18-Fluoride in a quaternary methyl ammonium (QMA) anion exchange column (in the synthesis module), elution of F-18-Fluoride from the QMA column by TBA or kryprofix solution, azeotropic drying, substitution reaction with the mannose triflate precursor, hydrolysis (acidic/basic), and purification of final product. After purification, the final product is passed through a 0.22  $\mu\text{m}$  filter and collected in a sterile vial.

The radiochemical purity (RCP) is a crucial quality control parameter, so it should be tested by approved and validated methods. The results of the test must meet the batch release criteria. The present study aims to explain the methods for determination of radiochemical identity and radiochemical purity (RCP) for F-18-FDG as per the United States Pharmacopeia (USP) and the European Pharmacopeia (EP) along with factors affecting the RCP of F-18-FDG and their resolution.

Radiochemical identity is the identification of the molecular structure of the product in which the radioactive compound is compared with a reference standard (cold compound). For the identification of F-18-FDG, it is compared with F-19-FDG using the chromatography method (Figure 1), and the obtained relative front or retardation factor ( $R_f$ ) value is compared.



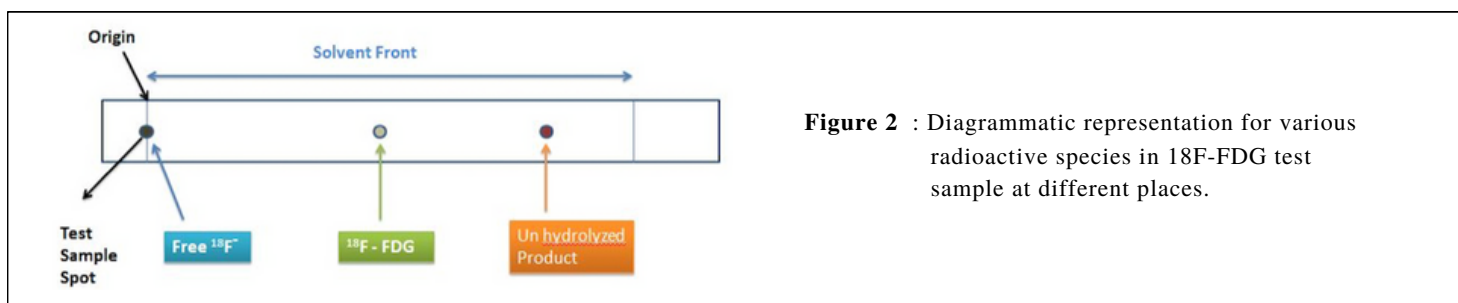
In USP, thin layer chromatography (TLC) method is recommended for the identification test. A test sample of F-18-FDG and the cold compound F-19-FDG should be applied to two silica gel TLC strips at the same distance from the origin front. The strips should be developed using 95:5 acetonitrile:water (v/v) as solvent. The  $R_f$  value of F-18-FDG and reference standard should be  $\sim 0.4$ .

However, in EP, no separate radiochemical identity test is defined. It is combined with a radiochemical purity test in which the product should have the same retention time as that of the reference standard in a high-performance liquid chromatography (HPLC) test.

Radiochemical purity can be defined as the fraction of total radioactivity present in the desired chemical form, or we can say it is a proportion of the total radioactivity in the sample that is present as the desired radiolabeled species.

As per USP, radiochemical purity can be determined by the TLC method, as reported earlier. The Rf of F-18-FDG should be ~0.4. The RCP should be greater than 90% in the final injection of F-18-FDG.

EP recommends two methods for evaluation of radiochemical purity of F-18-FDG, TLC and HPLC. In the TLC method, a silica gel TLC sheet is used as the stationary phase and a mixture of acetonitrile and water (95:5, v/v) as the mobile phase. Radiochemical purity should not be less than 95% in 18F-FDG injection and Rf of F-18-FDG should be 0.45 (Figure 2).



For HPLC method, the radioactivity of F-18-FDG and 2-F-18-fluoro-2-deoxy-D-mannose (F-18-FDM, an epimer of F-18-FDG) should not be less than 95% of the total radioactivity and the fraction of F-18-FDM should not exceed 10%. The stationary phase for HPLC analysis is an anion exchange column (Dionex CarboPack) and the mobile phase is a 0.1 mM/L Sodium hydroxide.

### IMPACT OF LOW RADIOCHEMICAL PURITY

Radiochemical purity is a very important element of any radiopharmaceutical. Every radiopharmaceutical has a specific biodistribution pattern. Reduced radiochemical purity may lead to an altered bio-distribution of injected radiopharmaceutical, compromising the image quality and resulting in a poor diagnosis. Low radiochemical purity also reduces the target to non-target ratio during the uptake and increases the radiation dose to the patient. Sometimes because of low radiochemical purity of injected F-18-FDG, a repeat scan may also be required.

In F-18-FDG, mainly three kinds of radiochemical impurities are defined, i.e., free or unreacted fluoride ion, un-hydrolysed or acetylated F-18-FDG and F-18-FDM (Epimer of F-18-FDG).

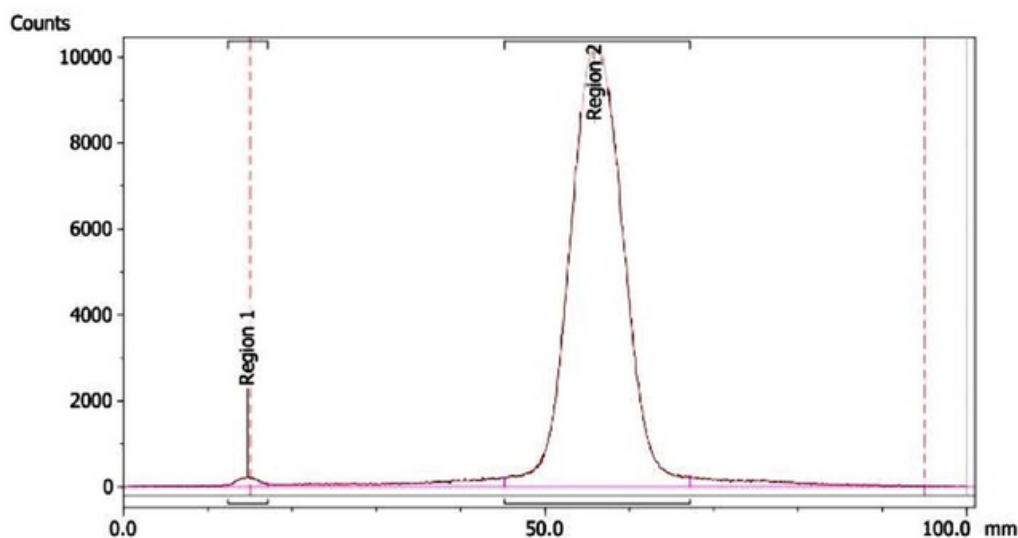


**Figure 3** : A normal TLC chromatograph of 18F-FDG test sample.

## FACTORS AFFECTING RADIOCHEMICAL PURITY

Most common factor that affects the radiochemical purity of a radiopharmaceutical is its radioactive concentration (activity/mL). High radioactive concentration leads to radiolysis in the final product resulting in a decrement of RCP. Data available in the literature regarding the impact of radioactivity strength on radiochemical purity is insufficient. However, no significant radiolysis effect has been observed on the F-18-FDG RCP for concentrations up to 200 mCi/ mL, till eight hours. Beyond this radioactive concentration, increase in radiolysis have been noted with increasing concentration and after eight hours considerable drop in radiochemical purity is observed. To avoid or minimize the radiolysis in final product, 0.1-0.3% ethanol can be added. It significantly reduces the radiolysis effect in 18F-FDG and aids in achieving the USP RCP recommendation for up to eight hours.

Insufficient purification can also be a reason for suboptimal radiochemical impurity. Usually purification columns are capable to hold the maximum impurities during purification step but sometimes inappropriate column conditioning or bad synthesis reaction or both may increase the breakthrough of impurities in the final product.

Epimerization of F-18-FDG to F-18-FDM may also be a cause for low radiochemical purity. Acidic hydrolysis reduces the potential of epimerization of F-18-FDG to F-18-FDM. Epimerization reaction is dominant in alkaline hydrolysis at high temperature but in most of the automatic synthesis modules alkaline hydrolysis has been performed at room temperature, reducing the possibility of conversion of F-18-FDG to F-18-FDM to almost negligible.

A part from the above mentioned reasons, delay in time of injection from the end of synthesis also plays an important role in degradation of RCP. As the time increase there is a possibility of decrement in the radiochemical impurity. We have also noticed that sometimes mechanical (hardware) and software malfunctioning during synthesis are also potential reasons for reduced radiochemical purity.





## Silver ion-exchange resin to reduce the volume of eluted Re-188-perrhenate from W-188/Re-188 generator for synthesizing Re-188-radiopharmaceuticals

Anupriya Chhabra, Jaya Shukla, Yogesh Rathore, Rakhee Vatsa, Bhagwant Rai Mittal

*Department of Nuclear Medicine, Postgraduate Institute of Medical Education and Research-160012, Chandigarh*

### Background

Rhenium-188 (Re-188) is a beta and gamma-emitting theranostic radionuclide. It has  $E_{\beta\text{max}} = 2.12$  MeV and  $E_{\gamma} = 155$  KeV (15%). The  $t_{1/2}$  is 16.9 h, and the maximum and mean tissue penetration are 11 mm and 3 mm, respectively. Re-188- tagged radiopharmaceuticals are widely used for radionuclide therapies to treat liver cancers, keloids, skin cancer and bone pain palliation [1, 2].

Rhenium-188 can be obtained in the form of Re-188-perrhenate from the Tungsten-188/Rhenium-188 (W-188/Re-188) generator. The generator system is based on the chromatographic system. Tungsten-188 is adsorbed on the alumina column with a high partition coefficient (Kd) and decays continuously to Re-188. Using 0.9% saline as a mobile phase, Re-188 can be eluted. Tungsten-188 is produced in a reactor and often has a very low specific activity. To obtain maximum activity, a large volume (8-14 mL) of 0.9% normal saline is required for elution [3]. Moreover, the amount of Re-188 available from the generator decreases each day as a result of the decay of W-188. The decrease in activity per unit volume affects the radiochemical yield. The preparation of various Re-188-labeled radiopharmaceuticals such as Re-188-HEDP, Re-188-HDD, and Re-188-colloid requires small volumes of  $^{188}\text{Re}$  for achieving high radiochemical yield. Therefore, the concentration of Re-188 in low volume (~1 mL) is of prime importance [4-6].

The present study describes the application of a silver ion exchange resin column to concentrate the Re-188-perrhenate eluted from the W-188/Re-188 generator

### Concentration Protocol

Silver ion exchange resin (5 g, AG-50) dissolved in 0.5 M silver nitrate was stirred for 3-4 h on a magnetic stirrer, followed by incubation at room temperature for 30 h. Two set-ups were used to concentrate the Re-188-perrhenate. In the first set-up, a glass column was fixed to a stand, and the outlet was closed with a cap (Figure 1a). In the second set-up, a 10 mL syringe was used as a column. The plunger was removed, and glass wool was inserted inside to block the nozzle (Fig.1b). The soaked resin was poured inside the glass column/syringe and washed with 15-20 mL HPLC grade water (flow rate 1 mL/min) until a clear solution was eluted.

To avoid radiation exposure to the personnel performing the procedure, all the work should be done behind the lead shielding. Re-188 was eluted from the W-188/Re-188 generator with 0.9% normal saline. The volume of saline was used as per the manufacturer's instruction manual for W-188/Re-188 generators.



For the present study, 8 mL and 14 mL of 0.9% normal saline were used for the PARS and ITG generators, respectively. The eluted Re-188 was passed onto the column at a flow rate of 1 mL/min. When elution was done with the tubing system, the generator output line was connected to the glass column (Figure 1c) to pass the eluted Re-188-perrhenate onto the resin column directly. The chloride ions present in the saline (elution solution) precipitated with the silver present in the resin and remained trapped in the column. However, Re-188 passed through the resin beads, eluting out of the column, and was collected in a clean, sterile glass vial.

The Re-188 solution eluted from the resin column was then passed through the quaternary methyl ammonium (QMA) cartridge to trap Re-188 ions via an anion exchange mechanism. The solution was collected in a vial, and the activity associated with it was measured. Normal saline (1 mL) was passed through the QMA cartridge for eluting the trapped Re-188. For each experiment, the QMA cartridge was used only once. To ensure the sterility, Re-188 was passed through a 0.22 µm filter (Fig. 1a).

The percentage yield was calculated as the ratio of activity obtained in 1 mL saline to the total activity eluted from the generator.

$$\text{Yield (\%)} = \frac{\text{Activity obtained in 1mL saline}}{\text{Total activity eluted from the generator}} * 100$$

Greater than 98% of the eluted 188Re perrhenate was observed to be recovered in 1 mL of normal saline. The concentration system could reduce volume up to 1/14th time.

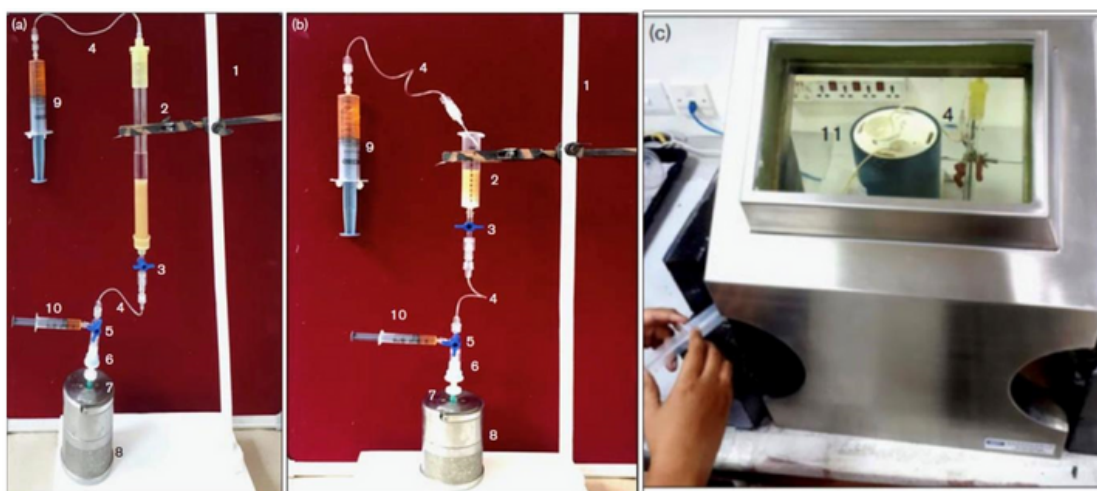


**Figure 1** : Re-188 concentration assembly showing (a) Silver ion exchange resin loaded in a glass column (b) Precipitation of silver chloride on the resin in the syringe. (c) assembly attached directly to the generator behind the lead 'L' bench [7]. Note: Colour in syringe is to illustrate fluid.

### Quality Control of Concentrated Rhenium-188

The quality control of concentrated Re-188 was performed as per standard procedures. Concentrated Re-188 solution was colourless with pH between 6.0-7.0. Retardation factor (Rf) in saline and acetone was 1.0 as observed in radio-thin layer chromatography. The concentrated Re-188 solution was observed to be sterile on sterility test. Endotoxins levels were well within the permissible limit 0.1-0.25 EU/mL (limit 175 EU/V; V=maximum volume of injection), with spike recovery > 60% (acceptable range 50-200%).

The concentrated Re-188 was observed to be suitable for the preparation of various high-yielding Re-188-labeled radiopharmaceuticals. Silver ion exchange columns are suitable for facile concentration of Re-188-perrhenate in a hospital based radiopharmacy set up.

## REFERENCES

1. Argyrou M, Valassi A, Andreou M, Lyra M. Rhenium-188 production in hospitals, by W-188/Re-188 generator, for easy use in radionuclide therapy. *Int J Mol Imaging*. 2013;290750.
2. Knapp FF. Rhenium-188 a generator-derived radioisotope for cancer therapy. *Cancer Biother Radiopharm*. 1998;13:337-49.
3. Guhlke S, Arnold L, Oetjen K, Mirzadeh S, Biersack H, Furn F. Simple new method for effective concentration of Re-188 solutions from alumina based W-188/Re-188 generator. *J Nuc Med*. 2000;41:1271-1278.
4. Mallia MB, Shinto AS, Kameswaran M, Kamaleshwaran KK, Kalarikal R, Aswathy KK. A freeze-dried kit for the preparation of Re-188 -HEDP for bone pain palliation: Preparation and preliminary clinical evaluation. *Cancer Biother Radiopharm*. 2016:139-144.
5. Shukla J, Bandopadhyaya GP, Shamim SA, Kumar R. Characterization of  $^{188}\text{Re}$ -Sn microparticles used for synovitis treatment. *Int J Pharmaceutics*. 2007; 338:43-47.
6. Kumar A, Bal C, Srivastava D, Acharya S, Thulkar S, Sharma S. Transarterial radionuclide therapy with  $^{188}\text{Re}$ -HDD-lipiodol in case of unresectable hepatocellular carcinoma with extensive portal vein thrombosis. *Eur J Radiol*. 2005;56:55–59.
7. Chhabra A, Rathore Y, Bhusari P, Vatsa R, Mittal BR, Shukla J. Concentration protocol of rhenium-188 perrhenate eluted from tungsten-188/rhenium-188 generator for the preparation of high-yield rhenium-188-labelled radiopharmaceuticals. *Nucl Med Commun*. 2018; 39:957-959.



## A cost-effective single step purification method for in-house conjugated and radiolabeled small peptide in absence of semi-preparative HPLC

Gurvinder Kaur, Somit Pandey, Rakhee Vatsa, Jaya Shukla, BR Mittal

Department of Nuclear Medicine, Postgraduate Institute of Medical Education and Research, Chandigarh



### INTRODUCTION

Development of radiopharmaceutical, with radio-metals in particular, involve the covalent attachment (conjugation) of peptide with linear or cyclic bifunctional chelating agents (BFCA) such as 2,2',2''-(1,4,7-triazacyclononane-1,4,7-triyl) triacetic acid (NOTA), 1,4,7,10-tetraazacyclododecane-1,4,7,10-tetraacetic acid (DOTA), 2,2',2''-(10-(2,6-dioxotetrahydro-2H-pyran-3-yl)-1,4,7,10-tetraazacyclododecane-1,4,7-triyl)triacetic acid (DOTAGA), N,N-bis(2-hydroxybenzyl) ethylenediamine-N,N-diacetic acid (HEBD), and diethylenetriaminepentaacetic acid (DTPA). Bifunctional ligands are the reactive moieties that can effectively encapsulate the radio-metal and have a reactive functionality, usually an aromatic isothiocyanate group or an activated ester, which will react with nucleophilic sites (-NH<sub>2</sub>, -SH, or -OH) of the targeting peptide as shown in figure 1. The commonly practiced technique for cross-linking the peptides involves the use of chemical groups that react with primary amines (-NH<sub>2</sub>). Primary amines are positively charged at physiologic pH; therefore, they occur predominantly on the outside surfaces of native protein tertiary structures and are readily accessible to conjugation reagents when introduced into an aqueous medium.

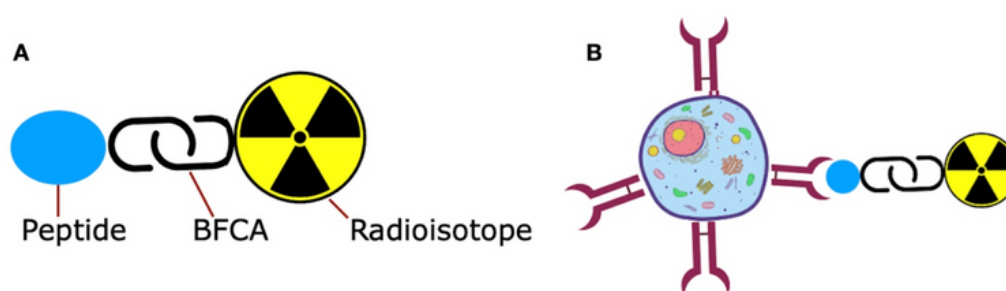


**Figure 1** : Schematic diagram showing (A) Bifunctional chelating agent (BFCA) attached to peptide at one end and to radio-metal at other, (B) Binding of radiopharmaceutical to over expressed receptors.

The chemical condition employed for conjugation with appreciable yield requires use of excess molar ratio of chelating agent in comparison to the peptide (>1:2). Presence of the excess leftover chelating agent during the radiolabeling step reduces the radiochemical purity of final product. Greater than 95% radiochemical purity (RCP) is recommended for injectable radiopharmaceutical. The reduced RCP may change the biodistribution pattern of radiopharmaceutical and increase the radiation burden to patient. In routine practice, after conjugation, the crude reaction mixtures are subjected to semi-preparative high performance liquid chromatography (HPLC) purification for removal of excess chelating agent. A second purification step is often required post radiolabeling to separate radiolabeled peptide from unbound radionuclide and radiolabeled chelating agent. However, the availability of semi-preparative HPLC, cost, and time involved for standardization of procedure are major limiting factors for this technique. The requirement of two step purification (after coupling of BFC with peptide and radiolabeling of the conjugated molecule) further complicates the process. There is ample scope for developing and optimizing a cost effective, easily available single step procedure for purification without HPLC.

In the present study, p-NCS-Bz-NOTA (NOTA) was conjugated with duramycin, owing to its ability to form thermodynamically stable and kinetically inert complex with gallium-68 ( $^{68}\text{Ga}$ ). Further purification using solid phase extraction (SPE) based method was optimized.

### **Duramycin Conjugation with NOTA**

In this study, conjugation of duramycin (2 kD, 19 amino acid lantibiotic) was optimized with NOTA followed by radiolabeling with gallium-68 ( $\text{Ga-68}$ ). The primary amine ( $\text{NH}_2$ ) of lysine in duramycin was targeted for conjugation with the isothiocyanate group of NOTA. For conjugation, different combinations of reaction conditions were tested, including molar ratio of peptide to BFCA (1:2-1:25), conjugation pH (7-10), incubation temperature, and incubation time. The reaction pH was maintained by phosphate buffer saline (PBS) and sodium bicarbonate ( $\text{NaHCO}_3$ ) solutions.

The conjugation was characterized by MALDI-TOF. For the determination of conjugation yield and radiochemical purity, the crude reaction mixtures were subjected to radiolabeling with  $\text{Ga-68}$ . Briefly, duramycin (10  $\mu\text{g}$ ) in conjugation reaction mixtures was incubated with  $\text{Ga-68-Cl}_3$  (10 mCi) eluted in 4 mL 0.05 M HCl at  $95^\circ\text{C}$  for 10 min at 4.0 reaction pH [1, 2]. The conjugation yield and radiochemical purity were estimated with a radio-TLC scanner on the basis of the difference in retention times of radiolabeled components present in the mobile phase (sodium citrate 0.5 M) and the stationary phase (Whatman paper).

A maximum conjugation yield and radiochemical purity of 80-85% was obtained at 1:2 molar ratio of duramycin with NOTA. For removal of excess uncoupled  $\text{Ga-68-NOTA}$ , solid phase extraction purification technique was optimized.

### **Solid Phase Extraction using Sep-Pak cartridge**

Purification of  $\text{Ga-68}$  labeled NOTA coupled duramycin was standardized using routinely used Sep-Pak C18 cartridge. This solid phase extraction separation technique is based on the hydrophobicity of different components present in the sample. The more hydrophobic components get eluted with strong hydrophobic solvent and vice versa [3]. The cartridge was conditioned with 70% ethanol (5 mL) solution and equilibrated with HPLC water (10 mL) for wetting of column bed. The crude radiolabeled reaction volume was loaded on the cartridge and elution protocol was standardized for combination of different ethanol gradients with water (range: 2-90%) and elution volume (2-10 mL).

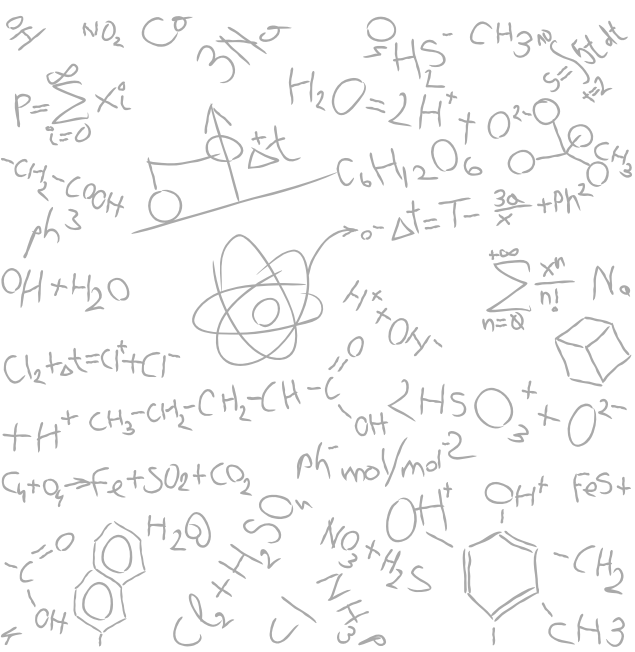
It was observed that the excess chelating agents ( $\text{Ga-68-NOTA}$ ) along with unbound  $\text{Ga-68}$  get eluted with 12-15% ethanol (10 mL). This was followed by elution of  $\text{Ga-68-NOTA-Duramycin}$  with >99% radiochemical purity with 1 mL 50% ethanol.

### **Conclusion**

A simple routinely adopted purification method has been standardized for single step purification of in-house conjugated and radiolabeled small molecules without the use of costly and tedious semi-preparative HPLC technique. This method can be further explored in research for easy purification of small radiolabeled molecules in nuclear medicine.

REFERENCES

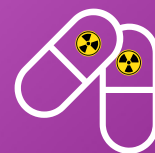
1. Sosabowski JK, Mather SJ. Conjugation of DOTA-like chelating agents to peptides and radiolabeling with trivalent metallic isotopes. Nat. Protoc. 2006; 1:972-976.
2. Delory GE, King EJ. A sodium carbonate-bicarbonate buffer for alkaline phosphatases. Biochem. J.1945; 39:245.
3. Baoshan S, Conceicao L, Jorge M, Ricardo S, Isabel S. Separation of Grape and Wine Proanthocyanidins According to Their Degree of Polymerization. J Agri Food Chem.1998; 46:1390-1396.



## Establishment of reference values for Tc-99m-Sulphur Colloid liquid meal whole gut transit scintigraphy

Suman, Naresh Kumar, Priyanka Gupta, Kh. Bangkim Chandra

*Department of Nuclear Medicine, AIIMS, New Delhi.*



### INTRODUCTION

Whole-gut transit scintigraphy (WGTS) is a single non-invasive technique that uses physiological meals and provides quantifiable and reproducible information in various clinical indications. It is simple, cost-effective, and easy to perform the study. Whole gut transit scintigraphy has been used to measure gastric emptying (GE), small bowel transit (SBT), and colonic transit (CT) after the oral administration of a radiolabeled meal [1].

Gastric emptying scintigraphy using solid meal is a physiological test which provides quantitative and reproducible information and is utilized to assess patients with gastroparesis symptoms. However, a good percentage of such patients may have normal solid meal gastric emptying. In such patients, additional evaluation of liquid meal gastric emptying might be beneficial. Moreover, many patients may have additional impairment of the small bowel and colonic transit. Hence, a single whole gut transit scintigraphy study assessing gastric emptying, small bowel transit, and colonic transit in the same sitting might be beneficial in selected patients from the diagnostic and management point of view for optimal patient outcome.

Whole gut transit has been assessed for liquid meal in the majority of the literature using a dual solid-liquid meal; the solid meal is labelled with Tc-99m-sulphur colloid (99mTc-SC) and the liquid meal with In-111-diethylenetriaminepentaacetate (In-111-DTPA) [2]. The effect of the solid meal on the derived values of the small bowel transit and colonic transit of a liquid meal is not known. Moreover, In-111 is not widely available and is associated with a higher radiation dose to patients as compared with Tc-99m. There is extremely limited data on assessment of whole gut transit using a single liquid meal than a dual solid-liquid meal. The reference values of whole gut transit using Tc-99m-SC labelled single liquid meal in the absence of a concomitant solid meal has not been established yet, to the best of our knowledge.

The current study aims to assess the whole gut transit (gastric emptying, small bowel transit and colonic transit) based on the easily available Tc-99m-SC which also has a favorable radiation profile.

### MATERIAL & METHODS

This is a prospective, non-interventional, analytical study conducted at the Department of Nuclear Medicine, AIIMS, New Delhi, over a 1-year duration from January 2022 to January 2023. A total of 35 healthy volunteers were included in this study. Patients with age < 18 years, pregnant or lactating women, pre-menopausal women >10 days of menstrual cycle and patient with diabetes or with any other conditions that might affect gastric emptying and intestinal motility (e.g., gastrointestinal illness or surgery, neurological illness) were excluded.

*Whole Gut Transit Scintigraphy Protocol*

All healthy volunteers fasted for at least 6 h before undergoing the procedure. Whole gut transit scintigraphy was performed on the healthy volunteers after they consumed a standard radiolabeled liquid meal containing 1 mCi of Tc-99m-SC within 5 min. The standard radiolabeled liquid meal consisted of 300 mL of potable water mixed with 1 mCi of Tc-99m-SC. Another 50 mL of potable water (non-radiolabeled) was taken immediately after the radiolabeled meal to wash any activity sticking onto the oropharyngeal region and esophagus. One-min static images encompassing the abdominal region were acquired at 0 h, 0.5 h, 1 h, 2 h, and 4 h post liquid meal consumption. Another delayed image was acquired after 24 h for 4 min, keeping the rest of the acquisition parameters similar to the previous acquisition. The acquisition was performed using dual head detectors simultaneously at each time point.

*Image Analysis*

Regions of interest (ROIs) were drawn, encompassing the gastric activity, entire abdomen, terminal ileum reservoir region, and entire abdomen in the anterior and posterior images for each time point imaging up to the 4 h image, each to calculate gastric emptying, the index of small bowel transit (ISBT), and the 24 h image to calculate colonic transit. The total gastric counts normalized to 100% for the time  $t=0$  (first image set immediately after meal ingestion).

The TIRC/TAC  $\times 100$  value represented the percent arrival of total small bowel activity at the terminal ileum and beyond at 4 h and was used as the index of SBT. An index of colonic transit at 24 h called colonic geometric center (CGC) was derived, which was given by the summation of decay-corrected counts at each region of interest (normalized to acquisition time) as a fraction of the decay-corrected total counts, weighted by that region number.

In simple terms,

$$\text{Colonic GC} = A/\text{TAC} \times 1 + B/\text{TAC} \times 2 + C/\text{TAC} \times 3 + D/\text{TAC} \times 4 + E/\text{TAC} \times 5$$

Where:

A = total activity of caecum-ascending colon at 24 h

B = total activity of transverse colon at 24 h

C = total activity of descending colon at 24 h

D = total activity of rectosigmoid-anal canal at 24 h

E = total activity eliminated in faeces at 24 h

TAC = total abdominal counts at 4 h

The values of CGC were calculated by both with geometric mean method and anterior view method. Further, the values derived on geometric mean method were also be compared to that derived on anterior view method.

**RESULTS**

A total of 35 consecutive healthy subjects (28 females, 7 males) with a mean age of  $42 \pm 11$  years (median 42; range, 23-65 y) were enrolled in the study. T<sub>1/2</sub> (half-time) of gastric emptying was calculated for 30 subjects as power exponential curve fitting was not feasible in the remaining 5 subjects. The 24 h imaging was performed in 22 subjects and hence CGC, also known as colonic transit parameter was derived only in these 22 subjects.

For each volunteer, a total of 12 images were acquired: 2 images immediately after meal, and 2 images each at 0.5 h, 1 h, 2 h, 4 h, and 24 h respectively, wherein each set of 2 images included anterior and posterior views. Anterior and posterior projections were used for geometric mean image analysis (Figure 1).

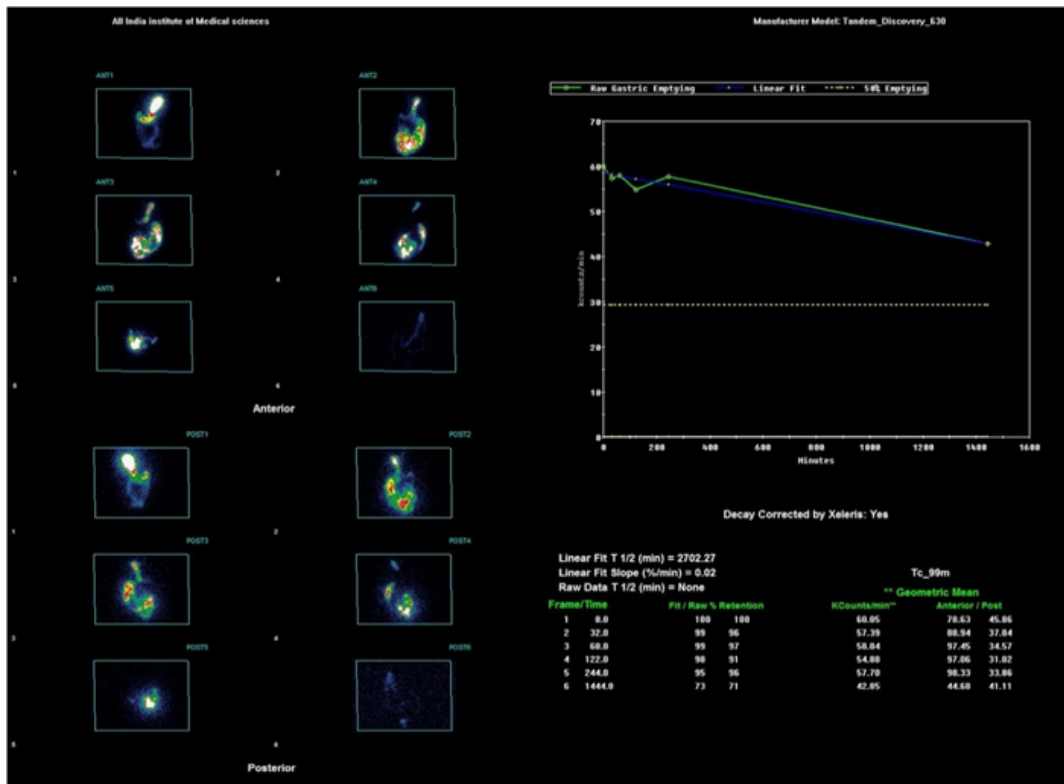


**Figure 1** :Representative image for calculation of time-activity-curve at 24 h using geometric mean method (anterior view, upper row; posterior view, lower row) in a 43-year-old healthy female volunteer. A large rectangular region of interest was drawn in both anterior and posterior images at 24 h encompassing the whole radioactivity in the abdomen region.

### Gastric Emptying Parameters of the Enrolled Subjects

- Anterior Method

The mean percent gastric retention (%) at 0.5 h, 1 h, 2 h, and 4 h were found to be  $39 \pm 18$ ,  $15 \pm 16$ ,  $5 \pm 10$ , and  $1 \pm 1$ , respectively, while the corresponding median percent gastric retention values were 40 (2-85), 9 (1-77), 1 (0-58), and 1 (0-4), respectively by anterior method. The mean T1/2 of gastric emptying was  $29 \pm 19$  min with a median value of 28 min (11-122). Summary statistics of gastric emptying parameters of the enrolled patients are depicted in Table-1.

- Geometric Mean Method

The mean percent gastric retention (%) at 0.5 h, 1 h, 2 h, and 4 h were found to be  $34 \pm 16$ ,  $13 \pm 12$ ,  $5 \pm 8$  and  $1 \pm 1$  respectively, while the corresponding median percent gastric retention values were 37 (2-72), 9 (1-52), 2 (1-45), and 1 (1-4) respectively, by geometric mean method. The mean T1/2 of gastric emptying was  $24 \pm 11$  min with a median value of 24 min (10-67). Summary statistics of gastric emptying parameters of the enrolled patients are depicted in Table-1.



*Index of Small Bowel Transit*

In the present study, the index of small bowel transit was derived as the representative small bowel transit parameter; and it was calculated on both anterior view and geometric mean methods.

*Comparison of Anterior View and Geometric Mean Methods*

According to the anterior view and geometric mean methods, the mean values of ISBT (%) at 4 h were 74±22 and 68±21, respectively; while the corresponding median values were 84 (25-94) and 77 (21-92), respectively. This difference was found to be statistically significant (P<0.001). Summary statistics of index of small bowel transit parameters of the enrolled patients are depicted in Table 1.

*Colonic Geometric Center*

In the present study, the colonic geometric center (CGC) was derived as the representative colonic transit parameter; and it was calculated on both anterior view and geometric mean methods. The raw parameters that were required as the necessary constituents for deriving the CGC were evaluated. These were caecum-ascending colon(C-AC), transverse colon (TC), descending colon (DC), rectosigmoid-anal canal (RS-AC) and eliminated activity (EA). These parameters were also calculated by both anterior view and geometric mean methods and were then compared. Summary statistics of colonic transit parameters of the enrolled patients are depicted in Table 1.

*Comparison of Anterior View and Geometric Mean Methods*

According to the anterior view and geometric mean methods, the mean values of CGC at 24 h were 3.1±0.8 and 2.4±0.7 while the corresponding median values were 3.3 (1.4-4.1) and 2.4 (1.2-3.8), respectively. This difference was found to be statistically significant (P<0.001).

**Table 1: Summary statistics of whole gut transit parameters**

| Parameter  | Mean<br>± SD | Median<br>(range) | Skewness | Kurtosis | Probability of<br>normality | Percentile        |                 |                  |                    |
|--|--------------|-------------------|----------|----------|-----------------------------|-------------------|-----------------|------------------|--------------------|
|  |              |                   |          |          |                             | 2.5 <sup>th</sup> | 5 <sup>th</sup> | 95 <sup>th</sup> | 97.5 <sup>th</sup> |
| <b>Gastric Emptying Parameters</b>                       |              |                   |          |          |                             |                   |                 |                  |                    |
| Percent gastric retention (%)<br>(Anterior view method)  |              |                   |          |          |                             |                   |                 |                  |                    |
| 0.5 h  | 39 ± 18      | 40 (2-85)         | -0.01679 | 0.3036   | 0.3302                      | 4                 | 7               | 69               | 80                 |
| 1 h  | 15 ± 16      | 9 (1-77)          | 1.8277   | 4.8699   | <0.0001                     | 1                 | 1               | 36               | 62                 |
| 2 h  | 5 ± 10       | 1 (0-58)          | 4.1982   | 19.6317  | <0.0001                     | 0                 | 1               | 23               | 46                 |
| 4 h  | 1 ± 1        | 1 (0-4)           | 1.8368   | 5.1696   | <0.0001                     | 0                 | 0               | 3                | 4                  |
| T <sub>1/2</sub> (min)                                   | 29 ± 19      | 28 (11-122)       | 3.8544   | 18.4373  | <0.0001                     | 11                | 11              | 46               | 103                |
| Percent gastric retention (%)<br>(Geometric mean method) |              |                   |          |          |                             |                   |                 |                  |                    |
| 0.5 h  | 34 ± 16      | 37 (2-72)         | -0.09666 | 0.07101  | 0.3458                      | 3                 | 6               | 59               | 68                 |
| 1 h  | 13 ± 12      | 9 (1-52)          | 1.1540   | 1.1268   | 0.0003                      | 1                 | 2               | 33               | 45                 |
| 2 h  | 5 ± 8        | 2 (1-45)          | 3.8082   | 16.4945  | <0.0001                     | 1                 | 1               | 20               | 37                 |
| 4 h  | 1 ± 1        | 1 (1-4)           | 1.6983   | 1.9904   | <0.0001                     | 1                 | 1               | 4                | 4                  |
| T <sub>1/2</sub> (min)                                   | 24 ± 11      | 24 (10-67)        | 2.0630   | 7.6095   | 0.0002                      | 10                | 10              | 40               | 60                 |

| Parameter                            | Mean<br>± SD | Median<br>(range) | Skewness | Kurtosis | Probability of<br>normality | Percentile        |                 |                  |                    |  |
|--------------------------------------|--------------|-------------------|----------|----------|-----------------------------|-------------------|-----------------|------------------|--------------------|--|
|                                      |              |                   |          |          |                             | 2.5 <sup>th</sup> | 5 <sup>th</sup> | 95 <sup>th</sup> | 97.5 <sup>th</sup> |  |
| <b>Small Bowel Transit Parameter</b> |              |                   |          |          |                             |                   |                 |                  |                    |  |
| ISBT (%)                             |              |                   |          |          |                             |                   |                 |                  |                    |  |
| Anterior view method                 | 74 ± 22      | 84 (25-94)        | -1.4552  | 0.7483   | <0.0001                     | 25                | 25              | 91               | 93                 |  |
| Geometric mean method                | 68 ± 21      | 77 (21-92)        | -1.3266  | 0.4980   | <0.0001                     | 21                | 23              | 86               | 90                 |  |
| <b>Colonic Transit Parameter</b>     |              |                   |          |          |                             |                   |                 |                  |                    |  |
| CGC                                  |              |                   |          |          |                             |                   |                 |                  |                    |  |
| Anterior view method                 | 3.1 ± 0.8    | 3.3 (1.4-4.1)     | -0.7926  | -0.2733  | 0.0800                      | 1.4               | 1.5             | 4.0              | 4.1                |  |
| Geometric mean method                | 2.4 ± 0.7    | 2.4 (1.2-3.8)     | 0.05068  | -0.7931  | 0.4187                      | 1.2               | 1.3             | 3.4              | 3.8                |  |

where, T<sub>1/2</sub>: half-time of gastric emptying; SD: Standard deviation; ISBT: Index of small bowel transit; CGC: colonic geometric center

*Establishment of reference values of whole gut transit*

In the present study, we proposed reference values of whole gut transit based on geometric mean method. Geometric mean method was used because this method includes both anterior and posterior image counts. The reference value of percent gastric retention at 0.5 h, 1 h, and 2 h was established as ≤60%, ≤33%, ≤20%, respectively, using 95th percentile values. On the basis of 95th percentile values, the reference value for half-time of gastric emptying was established as ≤40 minutes. The 5th percentile value for ISBT at 4 h was 23% hence, the reference value of ISBT at 4 h was established as ≥23% in geometric mean method. The reference value of CGC was established as 1.0–3.8. A value lower than the above-mentioned cut-offs may be regarded as delayed transit. A summary of reference values of whole gut transit based on the geometric mean method is depicted in Table 2.

**Table 2: Proposed reference values of whole gut transit parameters based on geometric mean method**

| Gastric Emptying Parameters |                   | Small Bowel Transit Parameter | Colonic Transit Parameter |
|-----------------------------|-------------------|-------------------------------|---------------------------|
| Time point                  | Percent retention | ISBT                          | CGC                       |
| 0.5 h                       | ≤60%              | >23%                          | 1.0 – 3.8                 |
| 1 h                         | ≤33%              |                               |                           |
| 2 h                         | ≤20%              |                               |                           |
| Half-time of emptying       |                   |                               |                           |
| ≤40 min                     |                   |                               |                           |

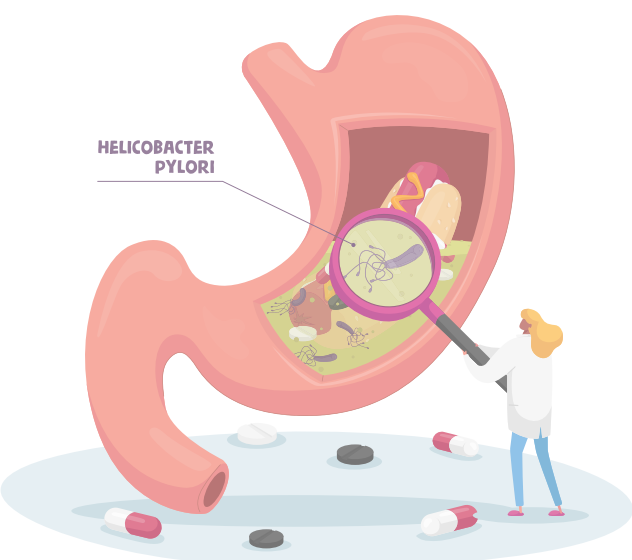
where, min: Minutes; ISBT: Index of small bowel transit; CGC: colonic geometric center

**CONCLUSION**

The study recommends the geometric mean method as the methodology of choice for assessing whole gut transit as attenuation correction was also incorporated. However, in very busy departments where one single-head gamma camera is used for multiple studies, the anterior view method can still be an acceptable alternative.

**REFERENCES**

1. Antoniou AJ, Raja S, El-Khouli R, Mena E, Lodge MA, Wahl RL, et al. Comprehensive radionuclide esophagogastrointestinal transit study: methodology, reference values, and initial clinical experience. *J Nucl Med.* 2015; 56:721-727.
2. Bonapace ES, Maurer AH, Davidoff S, Krevsky B, Fisher RS, Parkman HP. Whole gut transit scintigraphy in the clinical evaluation of patients with upper and lower gastrointestinal symptoms. *Am J Gastroenterol.* 2000; 95:2838-2847.



## DIGITAL SPECT-CT

Rakhee Vatsa

*Department of Nuclear Medicine, Advanced Centre for Treatment, Research and Education in Cancer  
Navi Mumbai, India*

Single photon emission computed tomography (SPECT) is a type of emission tomography in which the internal distribution of a radiopharmaceutical is determined by detecting the gamma photons emitted by the radiotracer with a single or set of collimated detectors. The gamma camera head/detector is rotated around the patient who has been injected with radiopharmaceutical, and data is acquired into a digital matrix at various angles (Figure 1). The detector heads can be operated either in continuous mode or step-and-shoot mode. The concept of SPECT was first introduced in the 1960s, and since the commercial arrival of SPECT systems in the 1970s, it has become a routine and important part of every nuclear medicine department. The main components of a SPECT system comprise a collimator, thallium-doped sodium iodide NaI(Tl) detector, an array of photomultiplier tubes (PMTs), electronic circuitry, and a pulse height analyser (Figure 2A). The hybrid SPECT systems also have computed tomography (CT) for anatomical localisation of various organs.

NaI(Tl) scintillation detector is the most commonly and widely used detector for gamma camera and SPECT/CT. However, a series of components and a complex chain of processes are involved in generating the required information from the scintillation signals produced by the detector. The use of PMTs increases the bulkiness of detectors. Also, periodic tuning of the PMTs is essential to ensure that the generated signals are of similar amplitude. Keeping in mind all these challenges, semi-conductor based solid state detectors have been considered as alternative detector material to NaI(Tl). Cadmium zinc telluride (CZT) has become the material of choice over cadmium, silicon, and germanium due to its high density (5.78 g/cm<sup>3</sup>), ability to perform at room temperature, and excellent detection efficiency for energetic photons.

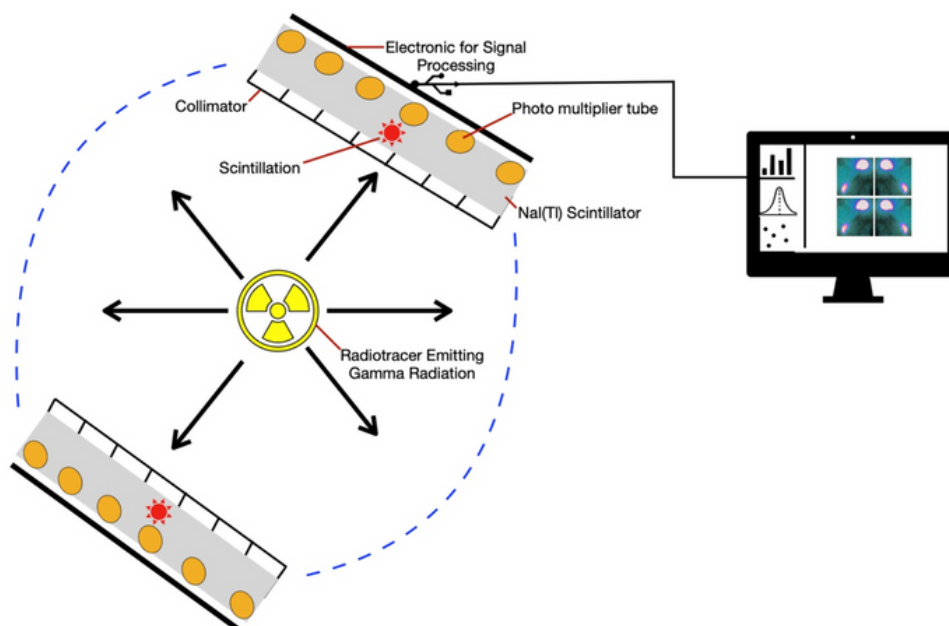


**Figure 1** :Schematic diagram image acquisition by a SPECT system.

The first CZT detector-based hand-held camera was commercially introduced by GE Healthcare for visualisation of sentinel lymph nodes for breast cancer patients. D-SPECT by Spectrum Dynamics became the first CZT based clinical system available on the market for cardiac perfusion SPECT imaging. The gamma photons, after interacting (photoelectric/Compton effect) with the CZT detector, create electron-hole pairs that are collected on the cathode and pixelated anodes. The absorbed energy of gamma photons can be directly converted to electrical signals and read by the detector's application specific integrated circuit (ASIC) as shown in Figure 2B. There is no need for intermediate amplification using PMTs. This is the main reason that the CZT-based systems are compact in size with increased sensitivity.

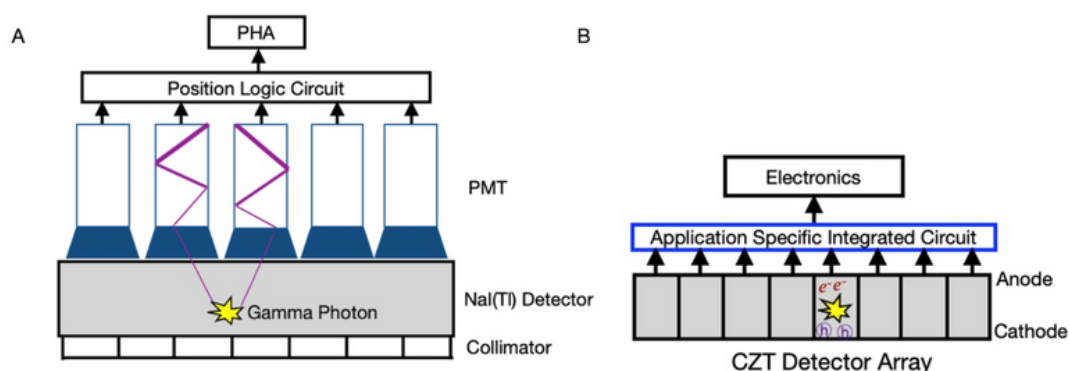


**Figure 2** :Schematic diagram showing (A) different component of a NaI(Tl) based, (B) CZT detector based SPECT system.

With the advancement in technology, CZT detector-based full SPECT/CT systems are now commercially available. Discovery NM/CT 670 CZT is a two-headed semiconductor based SPECT/CT system in which CZT detectors have replaced the NaI(Tl) detector and PMTs. The system is capable of imaging isotopes emitting low and medium energy gamma photons (Tc-99m:140 keV, Tl-201: 68-82 keV & 135 keV, I-123: 159 keV, and Lu-177: 113 keV & 208 keV).

Since the CZT detector-based cameras are capable of converting the gamma ray photons directly into digital signals, they are also known as digital SPECT. At present, three-dimensional whole body digital SPECT/CT systems having 360° detector configuration are available commercially. The two models currently on the market are the VERITON-CT by Spectrum Dynamics Medical (Figure 3A) and the Star Guide by GE Healthcare (Figure 3B). Some of the advantages of these systems are: 3D whole-body acquisition from head to toe in less time; increased sensitivity; better signal-to-noise ratio; and better detection ability of small lesions. Till now, these systems were able to image only low and medium energy gamma photons. However, recently in EANM 2022, a new model of the VERITON-CT 400 series digital SPECT/CT (Spectrum Dynamics Medical) was launched, which is also capable of imaging high energy gamma photons (I-131: 364 keV) along with medium and low energy gamma photons.

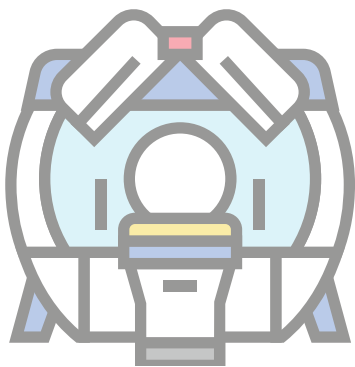


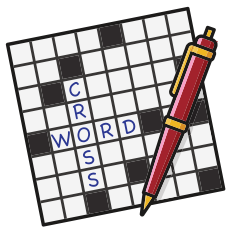
**Figure 3A** :Images of Spectrum Dynamics Medical: VERITON SPECT/CT.  
Images adapted from : <https://spectrum-dynamics.com/products/veriton-series>



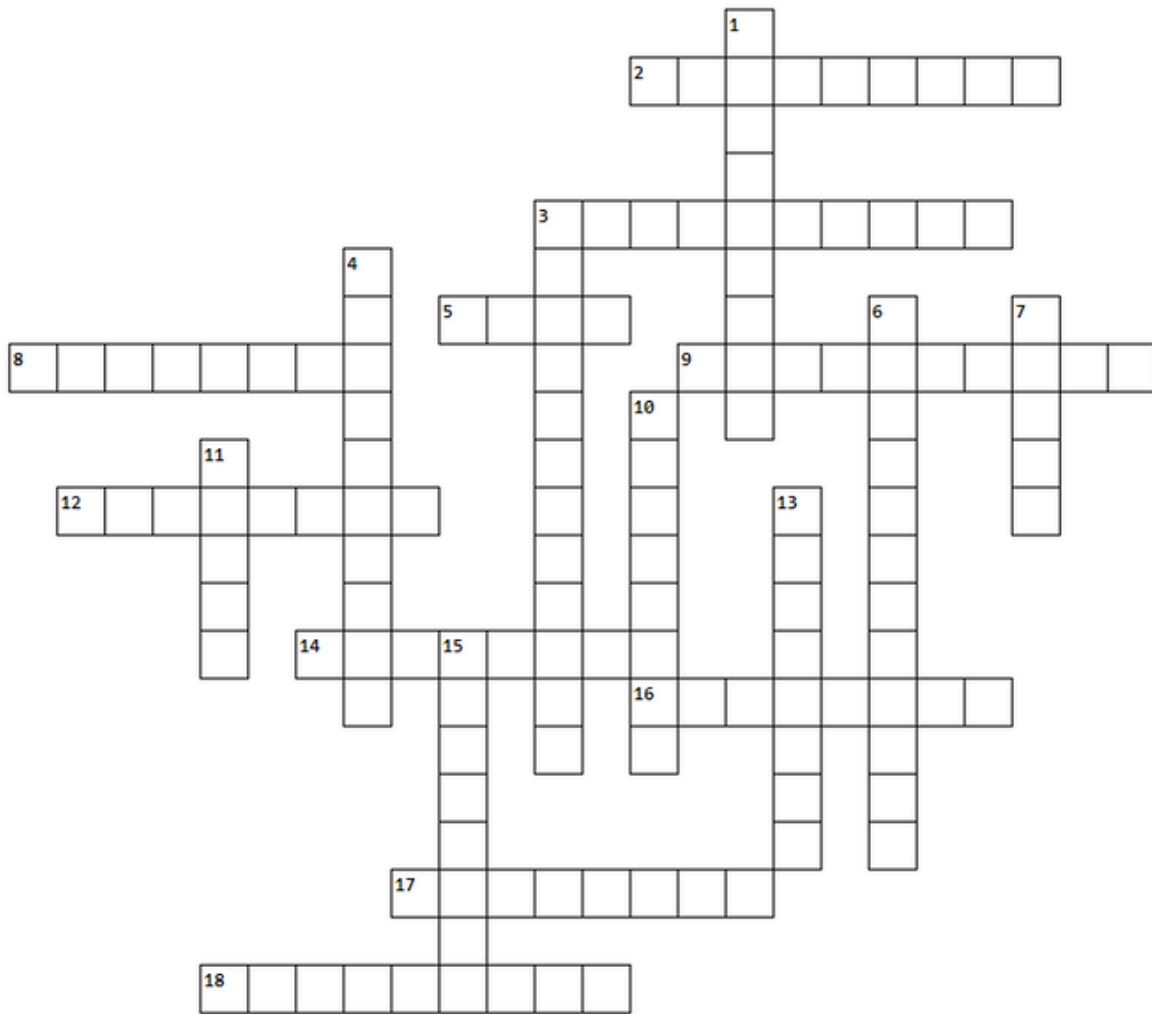
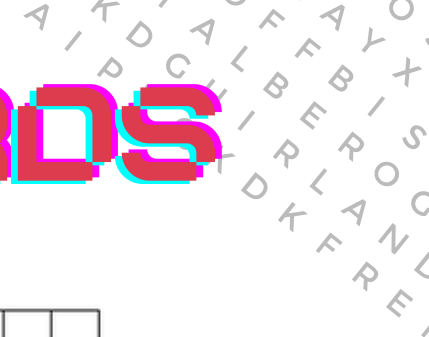
**Figure 3B** : Images of GE Healthcare: Star guide  
Images adapted from : <https://www.gehealthcare.com/products/molecular-imaging/starguide>

This state-of-art technology based systems will not only help in improving the image quality, but will also reduce the imaging time. The better image processing algorithms will definitely provide an upper edge over existing systems in terms of image quantification. The digital SPECT/CT systems seem to be a boon for research and dosimetry assessment studies. These systems may prove to be beneficial clinically and economically in long run.





# CROSSWORDS



## ACROSS

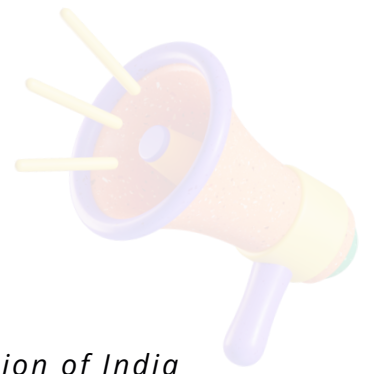
2. Stress agent in cardiac studies
3. Stable daughter product of Actinium-225 decay
5. Commonly used chelating agent
8. Nuclide used for splenic sequestration studies
9. Lightest element with all radioactive isotopes
12. Doping element/Impurity in NaI scintillator
14. Characteristic of Radionuclide
16. For better in-vivo stability of Ga-68 is labelled using which agent
17. Radiation exposure varies as Inverse Square of this factor
18. Most stable oxidation state for Technetium (2 Words)

## DOWN

1. SI unit of activity
3. Decay mode which results in increase in Z (2 Words)
4. Father of Indian Nuclear Medicine Program is
6. Process of conversion of masses into energy
7. Basic unit of image
10. Water radiolysis is an example of which effect radiation
11. Web-based application established by AERB used by Radiation Professionals for Registration
13. Commonly used leaving group in FDG synthesis
15. Bone seeking nuclide

ANSWERS IN NEXT ISSUE

# Schedule



## NATIONAL

### 7th Annual Conference of Nuclear Medicine Physicist Association of India

4-5 February, 2023

Mahamana Pandit Madan Mohan Malaviya Cancer Centre, BHU Campus,  
Varanasi, Uttar Pradesh

### Annual Conference of Society of Nuclear Medicine India (North Chapter)

8th April, 2023

Rajiv Gandhi Cancer Institute and Research Centre, New Delhi

Last date for Abstract Submission: Yet to be announced

### 21st Annual Conference of Association of Nuclear Medicine Physicians of India

29 September - 1 October, 2023

Sarvodaya Health Care, New Delhi

Last date for Abstract Submission: 31st August, 2023 (Tentative)

### 55th Annual Conference of Society of Nuclear Medicine India

7-11 December, 2023

AIIMS, Jodhpur

Last date for Abstract Submission: Yet to be announced

Upcoming Events



# Schedule



## INTERNATIONAL

12th International Symposium on Targeted Alpha Therapy

27 February - 2 March, 2023

Cape Town, South Africa

18th European Molecular Imaging Meeting

14-17 March, 2023

Salzburg, Austria

International Symposium on Trends in Recent Radiopharmaceuticals

17-21 April, 2023

Vienna, Austria

25th International Symposium on Radiopharmaceutical Chemistry

22-26 May, 2023

Honolulu, Hawaii

50th British Nuclear Medicine Society Annual Spring Meeting

22-24 May, 2023

Harrogate, England

53rd Annual Scientific Meeting of the Australian and New Zealand Society of Nuclear Medicine

26-28 May, 2023

Adelaide, South Australia

Last date for Abstract Submission: Yet to be announced

Annual meeting of Society of Nuclear Medicine and Molecular Imaging

24-27 June, 2023

Chicago, Illinois, USA

11th International Conference on Isotopes

23-27 July, 2023

Saskatoon, Canada

Last date for Abstract Submission: 15th February, 2023.

World Molecular Imaging Congress

5-9 September, 2023

Prague, Czech Republic

Last date for Abstract Submission: 17th April, 2023.

36th Annual Congress of the European Association of Nuclear Medicine

9-13 September, 2023

Vienna, Austria

Last date for Abstract Submission: 25th April, 2023.

Upcoming Events